Marine Pollution Bulletin 212 (2025) 117545

Contents lists available at ScienceDirect

Marine Pollution Bulletin

journal homepage: www.elsevier.com/locate/marpolbul

Seasonal changes in bay water column properties and their influence on the distribution of dissolved and particulate substances along the south coast of Curaçao (Caribbean Sea)

V. Sanchez Barranco [a,*], L. Schellenberg [b,c], F. Mienis [a], C.P.D. Brussaard [b,c], A.F. Haas [b], L.J. de Nooijer [a]

[a] Department of Ocean Systems, Royal Netherlands Institute for Sea Research (NIOZ), Texel, the Netherlands
[b] Department of Microbiology and Biogeochemistry, Royal Netherlands Institute for Sea Research (NIOZ), Texel, the Netherlands
[c] Institute for Biodiversity and Ecosystem Dynamics, University of Amsterdam, Amsterdam, the Netherlands

A B S T R A C T

As endpoints of watersheds, bays concentrate erosion- and human-derived substances such as dissolved inorganic nutrients and pollutants. We investigated the water movement and biogeochemistry of two bays in Curaçao: Piscadera Bay and Spaanse Water, during the dry (May 2022 and 2023) and wet seasons (November 2021 and 2023). Bay-ocean exchange was limited during the dry season, enhancing nutrient concentrations in the bays. The wet season showed increased mixing between bay and offshore water. Extreme rainfall from the 2023 El Niño event led to heavy runoff and wastewater influx, particularly in Piscadera Bay, where enriched $\delta^{15}N$ and total xenobiotic concentrations were over 1.5 times higher than in the dry season. Elevated $\delta^{15}N$ and $\delta^{13}C$ values reflected greater terrestrial influence in Piscadera Bay. These findings show how extreme weather, likely under future climate scenarios, can enhance nutrient and pollutant export from bays to reefs.

1. Introduction

Bays are partially enclosed coastal water bodies that connect terrestrial and ocean environments, often featuring a mix of fresh, nutrient-rich water from rivers or runoff and saline and oligotrophic water from the ocean (Gobler et al., 2005). Nutrient concentrations in bays depend on freshwater input, terrestrial runoff of sediments, pollutants and organic and inorganic matter and biological processes (Govers et al., 2014; Lapointe et al., 2011; Tuholske et al., 2021). Many bays in the Caribbean are heavily polluted, with high concentrations of nutrients, heavy metals and organic pollution, thereby posing a risk for nearby ecosystems within and around bays (Caballero-Gallardo et al., 2020; Govers et al., 2014; Siung-Chang, 1997). Poorly treated sewage water systems on some of the islands in the Caribbean cause a consequent anomalous high input of nutrients with frequently soaring concentrations in shallow coastal waters (Govers et al., 2014). This water with high nutrient- and substances-concentrations is often mixed with coastal water by processes such as tidal exchange, rainfall or mixing by wind (Gobler et al., 2005; Kjerfve and Magill, 1989), and can result in eutrophication of coastal waters (Wynne, 2017). Previous studies (Lao et al., 2022; Zheng et al., 2020) have shown that nearshore currents can transport pollutants released by bays over long distances, contributing to eco-environmental issues in coastal systems. This nutrient input reduces calcification rates and promotes the growth of macro-algae, disrupting the balance between benthic autotrophs and heterotrophs, posing a potential threat to the survival of tropical reefs (Fabricius, 2011).

The south coast of Curaçao is characterized by several inland bays that likely influence substances loads to the nearby shallow ecosystems such as coral reefs, mangroves and seagrass beds (Debrot et al., 1998; Wagenaar Hummelinck, 1977). As Curaçao lacks major rivers, most land-derived matter transport to the ocean occurs through submarine groundwater discharge, sewage systems, rainfall (Den Haan et al., 2016; Govers et al., 2014; van Sambeek et al., 2000) as well as the release from bays (Nagelkerken et al., 2005). The retention time of water in these bays determines to a large extent the adverse effects of terrestrial eutrophication and pollution loads on nearby coastal areas (Mestres et al., 2006). Chemical contaminants significantly impact marine biodiversity that can lead to reduction in species richness of up to 40 % (Johnston and Roberts, 2009). The molecular diversity of these contaminants has historically challenged monitoring their influx in marine systems (Hawkes et al., 2018). Untargeted metabolomics using liquid chromatography coupled with high-resolution tandem mass spectrometry (LC-MS/MS) is a powerful tool to detect a wide range of these

* Corresponding author.
E-mail address: virginia.sanchez@nioz.nl (V. Sanchez Barranco).

https://doi.org/10.1016/j.marpolbul.2025.117545
Received 11 November 2024; Received in revised form 7 January 2025; Accepted 8 January 2025
Available online 16 January 2025

chemical contaminants that can help characterizing the water composition of these bays. Eutrophication and pollution of bays in the Caribbean and mid-Atlantic coast have shown to cause detrimental impacts on coral reef ecosystems within and around the bays, such as enhancement of micro- and macro-algae causing light attenuation and affecting benthic photosynthesis processes, toxic algal glooms and disturbing herbivores nursery areas (Devlin and Brodie, 2023; Fabricius, 2011; Govers et al., 2014; Kennish, 2009).

Locally, ocean-bay exchange is modulated by rainfall, wind, geomorphological, hydrological and biochemical processes as well as hydrodynamic processes such as the transport and mixing of water masses, which control the distribution of dissolved and particulate substances on nearby fringing coral reefs (Hearn, 2011; Kjerfve and Magill, 1989; Odum, 1980; Sutula et al., 2003). Rainfall strongly differs between the wet (October–December with an average of 90.5 mm/month) and the dry season on Curaçao (April–June with an average of 8.2 mm/month) (Martis et al., 2001). Wind also affects sea surface water movement in shallow habitats (Adey and Steneck, 1985; D'Croz et al., 1999) and thus mixing of bay-derived water with the ocean. Surface currents and wind vary seasonally around Curaçao as well, with average lowest surface current velocities measured in October–November and highest speeds in December–March (Bertoncelj et al., 2024). Dominant trade winds in Curaçao are easterly and east-northeasterly winds, with speeds ranging from 5 to 8 m s^{-1}, with maxima from January to July and lower speeds from August to November (Hersbach et al., 2020). Therefore, the adverse effects of substances collected in, and exported from, bays to the coastal zone likely varies throughout the year. In addition, periods with higher pressure from tourism (December–April and June–August; (Thielman, 2013)) may result in seasonal variability in human-derived matter input in bays. While numerous studies have explored the influence of hydrological, geomorphological, and biochemical processes on bay-ocean exchanges (e.g., Odum, 1980; Sutula et al., 2003), there remains limited understanding of how these processes vary across seasons in tropical bays, particularly in the Caribbean.

This study aims to investigate the role of two bays in Curaçao with different adjacent land uses, Piscadera Bay and Spaanse Water, in the release of dissolved and particulate substances into coastal and adjacent reef areas during the wet and dry season. Specifically, we address the following research questions: (1) How do water properties as well as concentrations of inorganic nutrients and suspended particulate matter (SPM), vary along the axis of the bays and in adjacent open ocean areas? (2) What are the chemical fluxes of dissolved substances between the bays and coastal waters, and how do these fluxes differ between the wet and dry seasons? (3) To what extent do anthropogenic substances, such as pharmaceuticals, personal care products, and pesticides, contribute to the chemical composition of waters in bays and the nearby coast? We hypothesize that seasonal differences, such as increased rainfall and runoff during the wet season, lead to higher pollutant fluxes from the bays into adjacent coastal waters, with potential consequences for nutrient cycling and reef health. To answer these questions, we determined water properties, nutrient and SPM concentrations, and their carbon- and nitrogen-stable isotope compositions. Additionally, xenobiotic substances were assessed at selected stations using an untargeted metabolomics approach, providing insights into anthropogenic inputs and their potential impacts on adjacent reef ecosystems (Piwowarska and Kiedrzyńska, 2022).

2. Methodology

2.1. Study area

The island of Curaçao lies in the Southern Caribbean Sea (12° 10′, −68° 59′) and measures approximately 444 km^2. It currently (2023) harbors over 150.000 inhabitants and around 1.2 million (cruise) tourists visit the island annually. The study sites (Fig. 1) were visited in November 2021 (wet season, average rainfall of 77 mm/month) and May 2022 (dry season, average rainfall of 1 mm/month), coinciding with a moderate La Niña and in May (dry season, average rainfall of 4 mm/month) and November 2023 (wet season, average rainfall of 129 mm/month), coinciding with a strong El Niño event (Curaçao Weather, n.d.).

The bays studied were Piscadera Bay and Spaanse Water (Fig. 1). The former, situated at the west side of Willemstad, has a surface area of 0.75 km^2 (Govers et al., 2014) and the area around this bay is urbanized (Steward et al., 2024). It is also an important catchment area (16–17 km^2, Fig. 1.b) for the mid-west part of the island (with 5 inflow points, Fig. 1.b) and includes input from a wastewater treatment facility (Govers et al., 2014). Piscadera Bay has a relatively wide mouth (ranging from 76 m at its narrowest point to 105 m at its widest) and shallow entrance (i.e. <6 m deep). Reefs upstream and downstream present a low coral cover (0–13 %) (Sandin et al., 2022).

Spaanse Water, located at the east end of Willemstad is considerably larger than Piscadera Bay (approximately 3.2 km^2) and it has a mouth that is deeper (15 m water depth) and wider (ranging from 85 m at its narrowest point to 160 m at its widest). Near the mouth of Spaanse Water, reefs are present with a coral cover of 4–28 % (Sandin et al., 2022). This Watershed is surrounded by highly urbanized areas along the west side of the bay and more natural areas in the east (Steward et al., 2024). It is also surrounded by a larger catchment area (23–24 km^2) compared to that of Piscadera Bay, with 10 inflow points (Fig. 1.c).

2.2. Bay transects

Conductivity-Temperature-Depth (CTD) profiles along transects from inside the bay towards the open ocean were conducted on a small boat with a SBE9plus equipped with a Wetlabs FLNTU to measure turbidity and fluorescence (as an estimate for chlorophyll-a (Chl-a)) (Fig. 1). Sampling stations were positioned along the transect approximately every 100 m to capture any gradient in water properties and substance concentrations across the bay. This spacing allowed for a bay-wide (from most in land to the bay mouth) assessment of spatial variability in key parameters, such as salinity, temperature, and nutrient concentrations. We focused our sampling on the primary exchange pathways focusing on the areas where interactions between bay waters and the coastal environment are most pronounced. While logistical constraints limited sampling within the inner layers of the bays, the chosen transects provide a robust framework for capturing the processes driving bay-coast exchange. The downcast of the CTD profiles was processed with the software Sea-Bird data SBE 11plus. Piscadera Bay was sampled in spring 2022 and 2023 and autumn 2021 and 2023, and the transect consisted of 12–18 stations. At 6–8 stations water samples were collected (Fig. 1.d, S1). Spaanse Water was visited in spring and autumn 2023, conducting CTD measurements along a transect of 16 stations, of which 6 were used to collect water samples (Fig. 1.e). For the water samples, a 4 L Niskin bottle was attached to the top of the CTD to take samples at chosen depths (i.e. 1 m under the surface and 1 m above the bottom). The water samples were subsampled for inorganic nutrients, i.e., phosphate, ammonia, nitrate and nitrite (PO_4, NH_4, NO_3, NO_2 respectively), silicate (Si), dissolved inorganic carbon (DIC), dissolved organic carbon (DOC) and suspended particulate organic matter (SPOM). Solid phase extraction of dissolved organic matter (SPE-DOM) was done by running 1 L of 0.22 μm filtered sampling water acidified to a pH of 2 with trace metal grade HCl over a 200 mg bed mass Bond Elut-PPL resin in a 3 mL volume cartridge (Agilent 12,105,005) (Dittmar et al., 2008; Petras et al., 2017).

In May 2023, an Acoustic Doppler Current Profiler (ADCP, Nortek Signature) was deployed at the mouth (6 m depth) of Piscadera Bay, Curaçao, to measure current speed and characterize exchange of waters within the bay with those of the coastal zone. The ADCP recorded water speed over five days at 3 m above the sea floor and the average speed (0.023 ms^{-1}) and maximum speed (0.086 ms^{-1}) were used to calculate

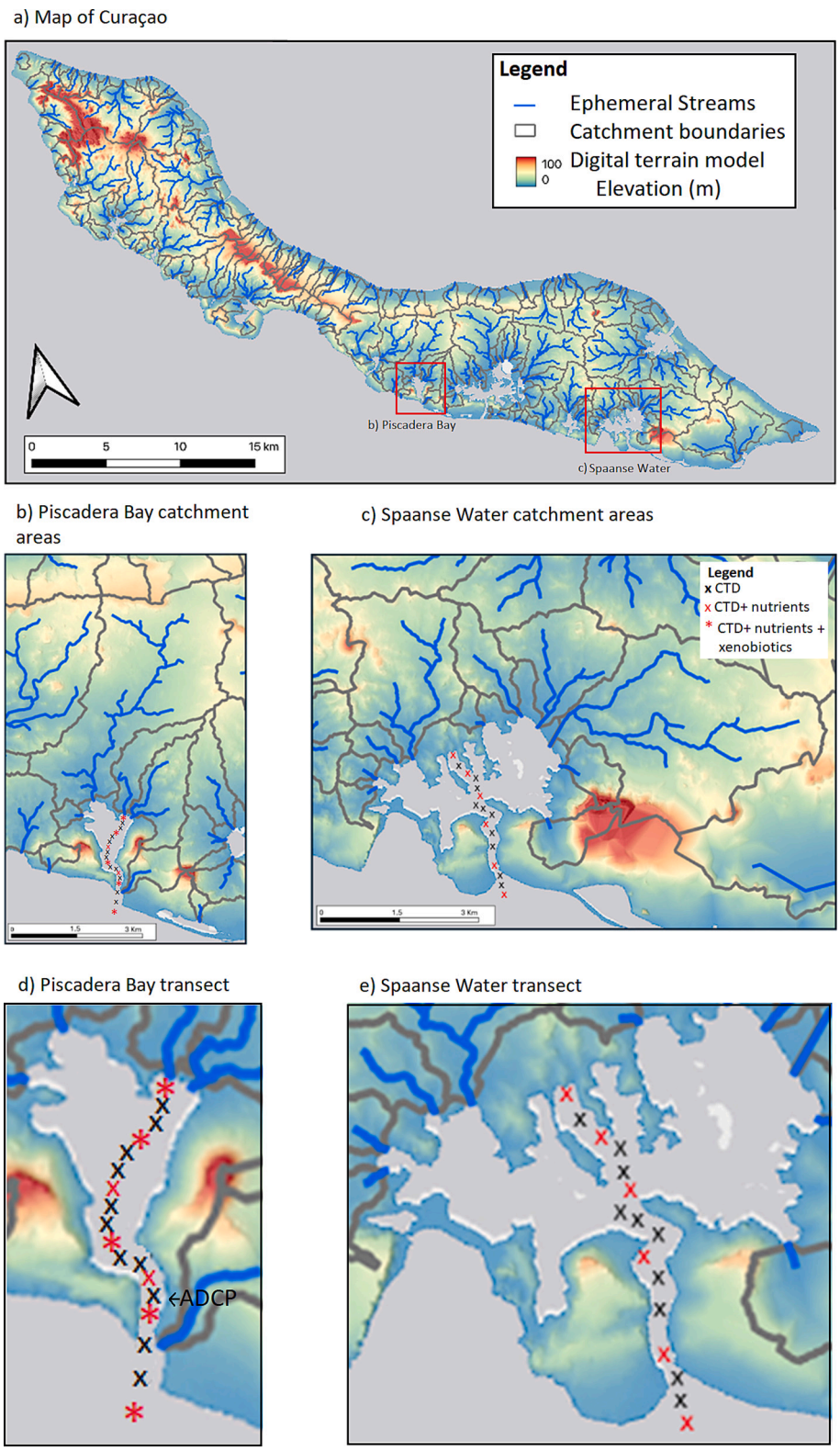

Fig. 1. Map of Curaçao a) and the catchment areas of the two sampled bays: Piscadera Bay b) and c) Spaanse Water. Map d) shows the transect conducted in Piscadera Bay including the ADCP location and e) in Spaanse Water. CTD stations are shown with black X, red X show the stations where nutrient water samples and red * where nutrient and xenobiotic water samples were taken (coordinates are summarized in S1). Maps were made in QGIS using an elevation model created by Titus Kruijssen. Stahler order 6 (i.e. size of the streams) was used to indicate the location of the streams. (For interpretation of the references to colour in this figure legend, the reader is referred to the web version of this article.)

substance fluxes following the method of Wang et al. (2022) and Kamjunke et al. (2023). The cross-sectional area of the mouth was estimated by multiplying the mouth's depth (6 m) by its average width (90 m), yielding a cross-sectional area of 540 m^2. Nutrient concentration gradients were calculated as the difference between nutrient concentrations in the bay and the adjacent ocean. Fluxes were estimated by multiplying the concentration gradient for each nutrient by the cross-sectional area and water velocity. The resulting nutrient transports were expressed in μmol s^{-1} L^{-1}, indicating the amount of nutrients transported from the bay to the ocean (positive values) or from the ocean to the bay (negative values).

2.3. Laboratory analysis

2.3.1. Dissolved inorganic nutrients

Water samples taken for dissolved inorganic nutrients, Si and DIC were collected using 50 mL syringes with a three-way valve and filtered through sterile 0.8/0.2 μm polycarbonate membrane syringe filters and collected in 6 mL high-density polyethylene pony vials. The samples were stored in a − 20 °C freezer (for analysis of PO_4^{3-}, NH_4^+, NO_3^- and NO_2) and a + 4 °C refrigerator (for Si). The DIC samples were collected in 6 mL polyethylene pony vials and 5 mL glass vials, respectively, containing 15 μL $HgCl_2$. DIC values were corrected for salinity with a reference salinity of 35 PSU (S2).

Inorganic nutrients concentrations were measured by using colorimetric analysis using a Bran & Luebbe TrAAcs 800 autonalyzer, following standard procedures (Grasshoff et al., 2009; Helder and De Vries, 1979b; Hydes et al., 2010; Murphy and Riley, 1962; Stoll et al., 2001; Strickland and Parsons, 1972a) with detection limits of approximately 0.02 μM for PO_4, 0.05 μM for NH_4, 0.01 μM for NO_2, 0.1 μM for NO_3, and 5 μM for DIC . A standard containing all inorganic nutrients was added to each run and used to monitor the performance of standards. All runs were calibrated with standards diluted in low nutrient seawater. DIC was measured photometrically with a QuaAAtro autoanalyzer (Seal Analyttical, Meqon, USA). Precision was ±10 mmol $kg\text{-}sw^{-1}$ based on recurrent measurements of an in-house standard that was calibrated against Batch No. 54 of A. Dicksons CRMS (Certified Reference Material Seawater, Marine Physical Laboratory, Scripps Institution of Oceanography). Measurements were made simultaneously on four channels for PO_4 (Murphy and Riley, 1962), NH_4 (Helder and De Vries, 1979a), and NO_{2+3} combined with NO_2 (Grasshoff et al., 2009) and separately for Si (Strickland and Parsons, 1972b). A freshly diluted mixed-nutrient standard containing Si, PO_4, and NO_{2+3} was added to each run. The cocktail served as a guide to monitor the performance of the standards. All measurements were calibrated with standards diluted in low nutrient seawater (LNSW).

2.3.2. Liquid chromatography tandem mass spectrometry (LC-MS/MS)

The 14 metabolomic samples from this dataset, including daily process blanks, were run in one sequential batch of a liquid chromatography tandem mass spectrometry following the method described in Petras et al. (2017). In brief, an aliquot (5 μL) of each sample, dissolved in methanol, was injected into a Ultra-high performance liquid chromatography system (UHPLC) (Agilent 1290 Infinity II), coupled to a Q-Exactive Plus Orbitrap Mass Spectrometer (Thermo Fisher Scientific, Bremen, Germany) equipped with an Ion-max source with a HESI (Heated Electrospray Ionization) probe. Chromatographic separation was performed with a C18 core-shell column (Kinetex, 150 × 2 mm, 1.8 um particle size, 100 Å pore size, Phenomenex, Torrance, USA), using solvent A: H_2O + 0.1 % formic acid (FA) and solvent B: Acetonitrile +0.1 % FA at a flow rate of 0.5 mL min-1. Samples were eluted using the following program: 0.5 min of 5 % B, followed by a linear gradient to 50 % B over 7.5 min, further followed by a 2 min gradient to 99 % B. This step is followed by a wash phase of 7 min at 99 % B and a re-equilibration at starting conditions for 8 min. Ion source was operated with the following settings: 70 AU sheath gas flow, 15 AU auxiliary gas flow, 0 AU sweep gas flow, Probe T 400 °C, spray voltage 3.5 kV, inlet capillary temperature, 320 °C, an S-Lens V of 50 V. The maximum ion injection time was 100 ms with automated gain control (AGC) targets of 1.0E6 for MS1 scans and 3.0E5 for MS/MS with a minimum threshold of 10 % C-trap AGC. Compounds were detected using a mass range of *m/z* 150–1500 with a resolution of 70,000 (at m/z 200) and one micro-scan per MS1. Fragmentation spectra were acquired in data dependent acquisition (DDA) mode of the 5 most abundant ions with a resolution of 17,500 (at m/z 200) with one micro-scan. A stepwise increased normalized collision energy from 20 to 30 to 40 % (z = 1 as default charge state) was used. The MS/MS experiments were triggered by apex of peaks with 2–15 s from first occurrence and the dynamic exclusion was set to 5 s with 3 ppm mass tolerance. Quality controls included a start and end sequence of injections of MeOH, Sulfa/Amih mix 0.01 μg/ul (STD6.1), MeOH, control seawater sample and MeOH injections between every 5 samples for monitoring.

2.3.3. SPOM, elemental analysis and isotopic ratios

Carbon and nitrogen isotopic composition (^{13}C and ^{15}N) of the samples taken in the bays were analyzed to constrain the source of the bays' organic matter. Seawater collected in Piscadera Bay and Spaanse Water were filtered using a vacuum pump over pre-weighed and combusted glass fiber filters (GF/F Whatman 1825–047). Subsequently, filters were freeze-dried, transported to The Netherlands and decarbonized with vapor of HCl (2 M). Processing and analysis were performed as described by Teece and Fogel (2004). An elemental analyser (EA) (Flash 2000 Elemental Analyser, Thermo Scientifc Bremen, Germany) coupled to an isotope-ratio mass spectrometer (Delta V Advantage Isotope Ratio Mass Spectrometer, Thermo Scientifc Bremen, Germany) via a Conflo IV was used to analyze the samples. The detection limits for this method are 0.011 mg for nitrogen and 0.035 mg for carbon. The Internationally recognized standards of acetanilide, urea and casein (Arndt Schimmelmann Biogeochemical laboratories, Indiana University) were used to calculate the isotopic composition. The isotope ratio $\delta^{13}C$ and $\delta^{15}N$ of the samples were obtained with the following equation: δX (‰) = (1) (R_{sample} /$R_{standard}$ − 1) * 1000, where δX is $\delta^{13}C$ or $\delta^{15}N$ and R is the isotope ratio $^{13}C/^{12}C$ or $^{15}N/^{14}N$ in the sample and in the standard, respectively. For the $R_{standard}$ Vienna PeeDee Belemnite (V-PDB; 0.0112372 ± 0.1 ‰) was used for carbon and air-N_2 (AIR-N_2; 0.003663 ± 0.15 ‰) for nitrogen.

2.4. Statistical and data analysis

To assess the spatial changes in the water column biogeochemistry along the transects of the bays, data were first tested for normality and equality of variance using a Shapiro-Wilk normality test. We used ANOVA tests to compare means of inorganic nutrients (PO_4, NH_4, NO_3, NO_2) and DIC concentrations between different locations along the bay transects (i.e. inner bay, mouth and open ocean). A *t*-tests was used to determine differences between samples collected in the dry and the wet season. Most of the suspended particulate matter samples collected at the mouth and at the open ocean near both bays during the dry season had nitrogen concentrations below the detection limit. CTD data and inorganic nutrient concentrations were visualized using the software Ocean Data View (Schlitzer, 2012).

Principal Component Analysis (PCA) was performed to determine the chemical similarity between water samples and their correlation to environmental parameters. Of all samples, 6 biochemical variables (Si, PO_4, NH_4, NO_2, NO_3 and DIC) in four seasons in Piscadera Bay (wet 2021, dry 2022, dry 2023 and wet 2023) and two seasons in Spaanse Water (dry 2023 and wet 2023) were used (S4). Seven environmental parameters (seawater temperature, fluorescence, depth, rainfall, location, tide and wind speed; S3) were used as explanatory variables to identify which one(s) may explain the biochemical variability in the data. The variables' location and tide are categorical, in the case of location 1 was assigned to bay samples, 2 to mouth samples and 3 to

open ocean and for tide 1 referred to neap and 2 to spring tide. All variables were auto-scaled and mean-centered for comparison. Eigenvalues were used to determine the contribution of the water biogeochemistry to the overall variance and as suggested by Shrestha and Kazama (2007), only Principal Components (PCs) with eigenvalues >1 are considered significant. Loadings were used to determine the contribution of each biochemical and environmental variables to the total variance of the biochemical water composition. Following Aydin-Onen et al. (2012) methodology, loadings were classified by strong (>0.75), moderate (0.75–0.5), weak (0.5–0.3) or insignificant (<0.3). In addition, a cluster analysis was used to group data into classes based on their biochemical composition. Hierarchical Agglomerative Clustering was performed using Euclidean distance to determine similarity and determine the preferable number of clusters with a 95 % confidence interval. All statistical analyses and graphing were performed in R (R-CoreTeam 2012) using RStudio (RStudioTeam 2015).

The data from liquid chromatography tandem mass spectrometry, was processed in MZmine3 (Schmid et al., 2023) followed by spectral matching with GNPS (https://gnps.ucsd.edu) (Wang et al., 2016) using the feature-based molecular networking workflow (FBMN, for details see S5 and S6) (Dittmar et al., 2008; Nothias et al., 2020). Final data clean-up and normalization was performed using a statistical pipeline designed specifically for Feature-based Molecular Networks from Non-Targeted Metabolomics Data by Pakkir Shah et al., (2024) (in review) where blanks were removed with a cut-off threshold of 0.3, allowing up to 30 % contribution from the blank and 70 % from the sample.

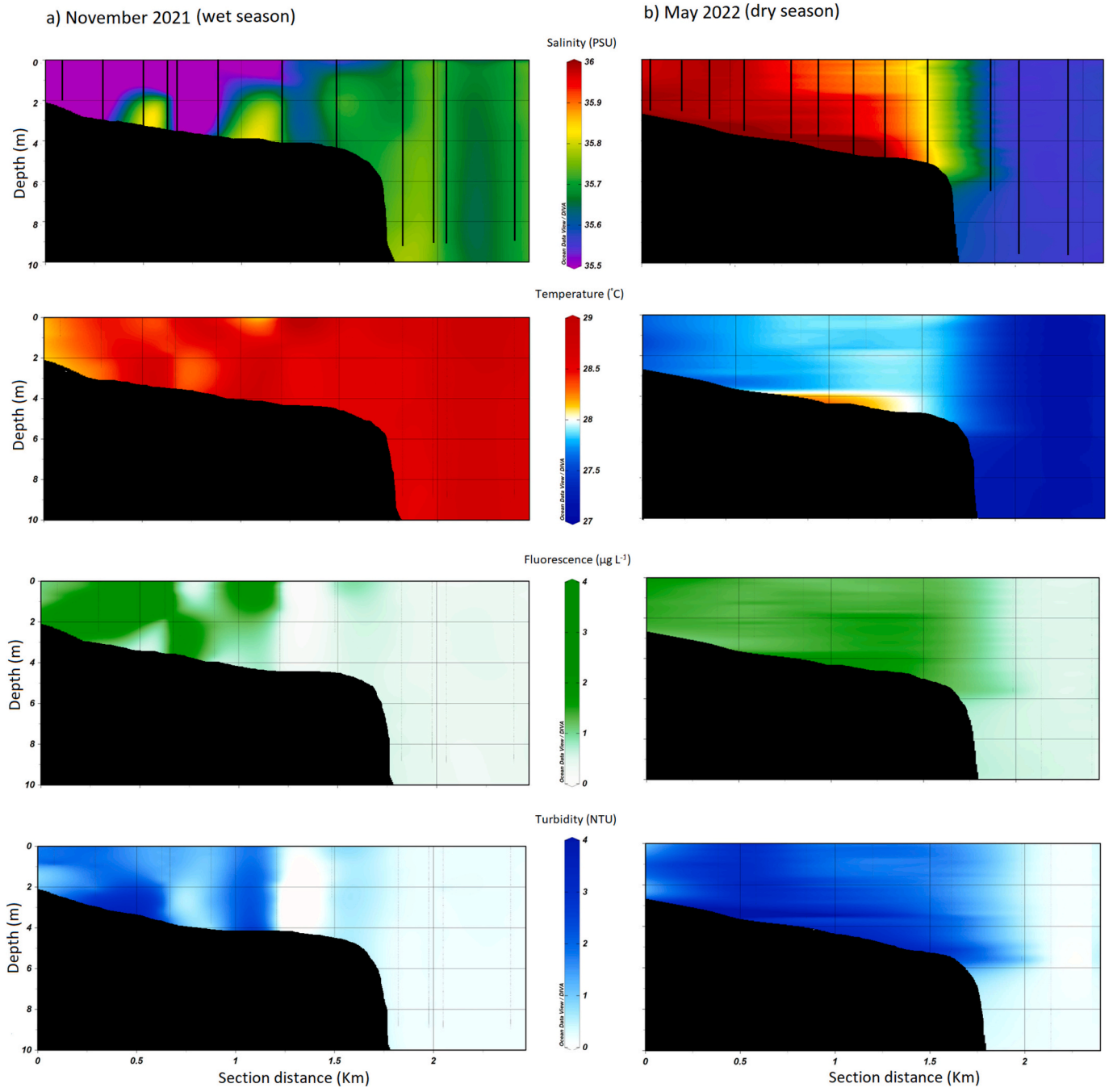

Fig. 2. Water column characteristics of Piscadera Bay in a) November 2021 (wet season) and b) May 2022 (dry season). From top to bottom, panels show Salinity, Temperature (°C), Fluorescence (µg L^{-1}) and Turbidity (NTU). Black vertical lines in the salinity panels show the 12 CTD profiles.

Xenobiotic substances were identified via the NORMAN Suspect List Exchange (NORMAN-SLE), a "living database" for suspect screening (Mohammed Taha et al., 2022). The database comprises subcategories of xenobiotics like: biocides, drinking water chemicals, drugs of abuse, food contact chemicals, human metabolites, human neurotoxins, indoor environment substances, industrial chemicals, natural toxins, persistent, mobile and toxic substances, personal care products, pharmaceuticals, plant protection products, plastic additives, smoke compounds,

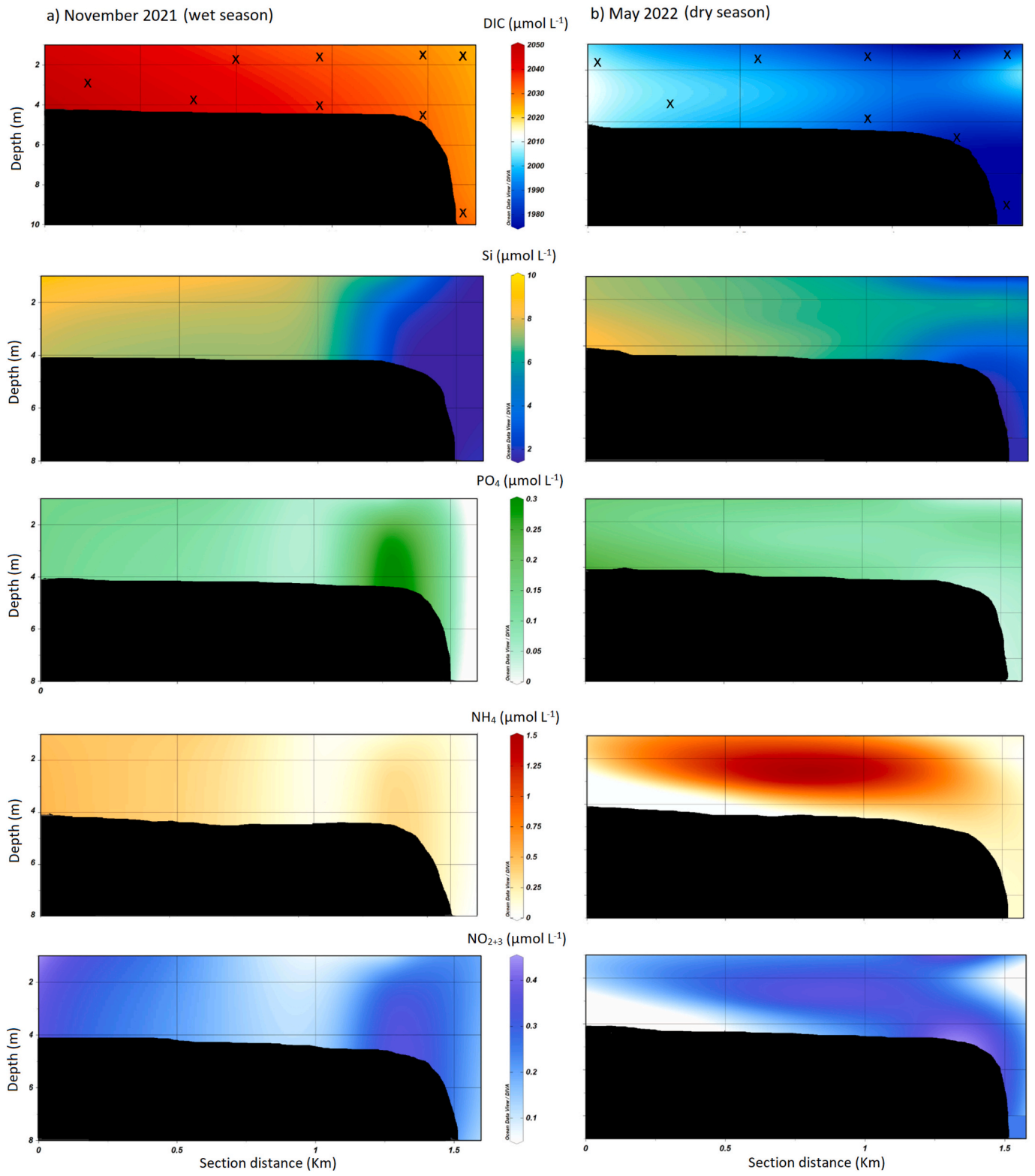

Fig. 3. Inorganic nutrient concentrations measured in Piscadera Bay in a) November 2021 (wet season) and b) May 2022 (dry season). From top to bottom, panels show DIC, Si, PO_4, NH_4, and NO_{2+3} (µmol L^{-1}). Crosses show the depths at which water samples were taken. Seasonal variations were evident across all measured parameters. DIC concentrations were significantly higher during the wet season, while NH_4 showed increased levels in the dry season. PO_4 and NO_{2+3} distributions varied spatially, with notable differences in vertical and horizontal concentration gradients between November and May.

surfactants. The InChIKey, which is a 27 character-condensed form of the international chemical identifier, was used to match hits between the NORMAN database and the annotated features derived from FBMN. R studio with R version 4.3.0 was used for coding, with the following packages: readxl, dplyr, openxlsx, readt, tibble, tidyverse, splitstackshape, pacman, svglite.

3. Results

3.1. Piscadera Bay seasonal dynamics in 2021–2022

Profiles of salinity, temperature, turbidity and fluorescence in Piscadera Bay differed between the wet (November 2021) and the dry season (May 2022; Fig. 2). During the wet season the surface of the inner bay was fresher (35.5–35.6), slightly cooler (28.2–28.5 °C), had higher fluorescence (3–4 μg L^{-1}) and turbidity (3–4 NTU) values compared to the open ocean (salinity~35.7; temperature~28.7 °C, fluorescence~0.48 μg L^{-1} and turbidity 0.3–0.7 NTU). In addition, bottom waters near the bay mouth were more saline (i.e. ~1 km from the inner point of the bay; Fig. 2.a). Piscadera Bay receives freshwater inputs primarily from rainwater runoff from its catchment area. Without a significant riverine input, the large catchment area contributes to nutrient loads, particularly during the wet season when rainfall is higher.

In the dry season (May 2022), a front was observed at the mouth of Piscadera Bay (Fig. 2.b) related to higher salinity (~36), and temperatures (27.9–28.1 °C) than the open ocean (salinity~35.6; temperature 27–27.2 °C). Fluorescence (2 μg L^{-1}) and turbidity (1–2NTU) were lower compared to the wet season, but still higher compared to values measured in the open ocean (fluorescence~0.5 μg L^{-1}, turbidity~0.2 NTU; Fig. 2.b).

Along the same transects, inorganic nutrients also differed between seasons (Fig. 3). Statistical analyses revealed significant differences in nutrient concentrations between seasons and locations. For NH_4 significant seasonal variations were observed (ANOVA, p-value = 0.002) with higher concentrations in May (1–1.5 μmol L^{-1}) compared to November (0.3–0.75 μmol L^{-1}). In November, NH_4 concentrations were similar along the transect (0.3–0.75 μmol L^{-1}; Fig. 3.a), matching the relatively uniform profiles for salinity and temperature (Fig. 2.a). DIC concentrations also differed significantly between seasons (ANOVA, p-value = 0.02). The wet season showed the highest DIC concentrations, coinciding with lower salinity and higher temperatures in both the bay and open ocean waters (Figs. 2.a and 3.a). In May, DIC concentrations were lower in the bay and open ocean (1980–2010 μmol L^{-1}), similar to surface ocean waters (1–3 m depth). Si however, showed less pronounced seasonal variations, with highest concentrations in the bay (November: 7–9 μmol L^{-1}; May: 6–8 μmol L^{-1}) gradually decreasing towards the open ocean (November: 2–3 μmol L^{-1}; May: 2–4 μmol L^{-1}).

Concentrations of PO_4 and NO_{2+3} were more variable in space. In November, concentrations of these nutrients were higher in the inner bay (0.12–0.16 μmol L^{-1} and 0.3–0.6 μmol L^{-1}, respectively), with enrichment in the top layer and increased concentrations at the bay mouth and open ocean. In May, the inner bay showed relatively high PO_4 concentrations (0.12–0.25 μmol L^{-1}), with elevated presence in the upper layers of the bay mouth and ocean (0.08–0.33 μmol L^{-1}). NO_{2+3} concentrations were highest in the upper layers of the bay and bay mouth (0.3–0.5 μmol L^{-1}), with lower concentrations deeper within the bay and open ocean (0.02–0.1 μmol L^{-1}).

3.1.1. Tandem mass spectrometry feature abundance in DOM

For the metabolomic analysis, a total of 29.113 unique ion features were extracted. By blasting these features against a curated database comprising >120,000 xenobiotic compounds we could identify 1638 features within the 8 stations taken during the two seasons in Piscadera Bay. The relative abundance of xenobiotics inside the bay was on average 1.7 times higher in the wet season compared to the dry season with season-distinct distribution patterns. During the wet season there was a visible gradient with highest concentrations (5-fold higher) at the landward end of the bay (Fig. 4.a). During the dry season abundance of xenobiotics was on average lower and relatively homogeneous throughout the bay (Fig. 4.b). Congruent to the other parameters assessed there was a clear drop in concentration from inside the bay to the surrounding ocean waters. In both wet and dry season, the majority of anthropogenically derived substances in the bay could be attributed to human metabolites, substances associated with indoor living spaces, surfactants, and pharmaceuticals. The only compound classes that were in higher abundance during dry than wet season were food contact chemicals (including pollutants from food packaging and processing and kitchen- and table utensils) and personal care products (Fig. 4).

3.2. Piscadera Bay and Spaanse Water seasonal dynamics in 2023

3.2.1. Environmental characteristics of the water column

The salinity, temperature, turbidity, and fluorescence profiles showed distinct spatial and temporal differences between Piscadera Bay and Spaanse Water (Fig. 5). Spatially, Piscadera Bay exhibited sharper gradients across its mouth compared to the more gradual transitions in Spaanse Water, particularly in May. Temporally, seasonal shifts were more pronounced in Piscadera Bay, with a strong front pesent in the dry season and absent in the wet season, while Spaanse Water demonstrated a more consistent mixing with the open ocean. Vertically, November profiles in both bays highlighted stratification, with warmer, fresher, and more biologically active surface waters overlaying denser, saltier, and less fluorescent deeper layers. These patterns suggest that local hydrography and mixing dynamics differ significantly between the two areas and between seasons.

In May, waters in Piscadera Bay were more saline (37–37.5), warmer (28–28.5 °C) and were higher in fluorescence (~1.6 μg L^{-1}) and turbidity (3–5 NTU) than the open ocean (where salinity was~36.7, temperature~26.5 °C; fluorescence~0.4 μg L^{-1} and turbidity~0.5; Fig. 5.a). As observed in the 2020's dry season, a front developed at the mouth in Piscadera Bay. In November, on the other hand, the inner part of the bay was less saline (35.0–35.5), warmer (30–31 °C), with higher fluorescence (4–6 μg L^{-1}) and lower turbidity (1–3), gradually becoming more saline, less warm and with less fluorescence towards the open ocean (Fig. 5). The obtained profiles of these parameters indicated more mixing between the bay and the open ocean (i.e. the front of 2021/2022 disappeared; compare Figs. 3 and 5). In addition, the top layer (~1 m) of the bay showed relatively high temperatures (~31 °C), low salinities (~34) and high fluorescence (5–8 μg L^{-1}) in November 2023.

CTD profiles collected in Spaanse Water showed similar patters as in Piscadera Bay (Fig. 5.b). In May, the inner bay water had a higher salinity (37.0–37.5), temperature (27–28 °C), slightly higher fluorescence (0.75–1.0 μg L^{-1}) and turbidity (0.50–1.5 NTU) compared to the open ocean (salinity~36.7; temperature 26.5–27 °C, fluorescence~0.4 μg L^{-1} and turbidity~0.3 NTU; Fig. 5.a). Compared to Piscadera Bay, there was no sharp change across the mouth of Spaanse Water (Figs. 5.a and 2.a). In November, conditions within the bay were similar to those of the open ocean (Fig. 5.b). The top 2 m of the bay's waters were characterized by lower salinity (34.0–34.5) and temperature (29.5 °C) and underneath this layer high salinity (35.5–36.0), temperature (30–31 °C), fluorescence (6–8 μg L^{-1}) and turbidity (4.5–5.0 NTU) were measured at the inner part of the bay.

3.2.2. Biogeochemical characteristics of the water column

Inorganic nutrients also varied along the transects (Fig. 6). Comparable to Piscadera Bay in 2021, average concentrations of DIC (2250–2400 μmol L^{-1}) and Si (20–40 μmol L^{-1}) were significantly higher in the bay during November (p-values <0.05, Fig. 6.a) compared to May (2050–2220 μmol L^{-1}; 8–14 μmol L^{-1}, respectively) and the highest values were measured at the surface (i.e. 1 m deep). However, DIC was 50–150 μmol L^{-1} and Si 10–30 μmol L^{-1} higher in November 2023 compared to 2021. PO_4 was also significantly higher in the bay

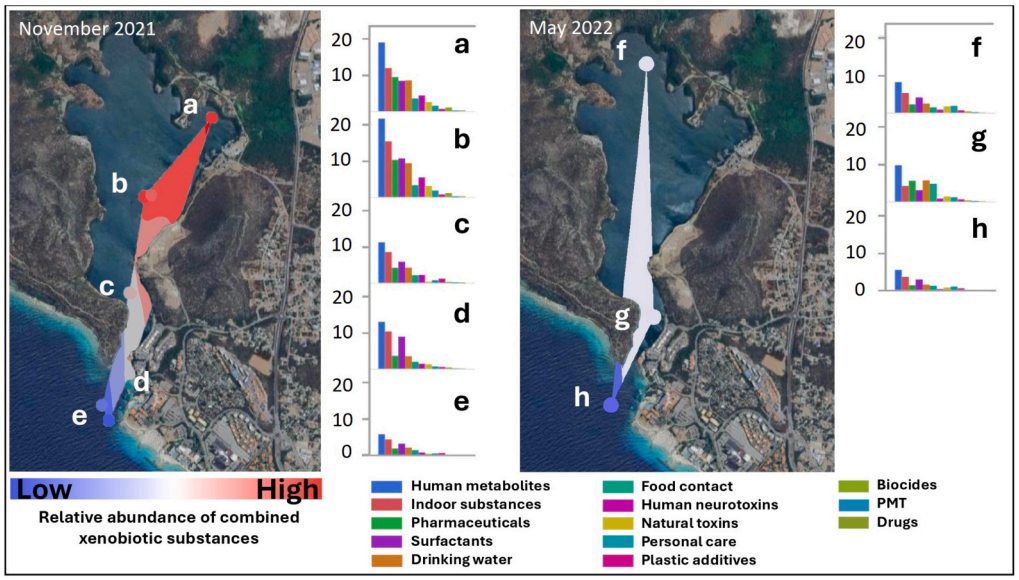

Fig. 4. Relative abundance of all detected xenobiotic substances throughout Piscadera Bay during wet season November 2021 (left) and dry season May 2022 (right). Bar charts show the relative abundance of different subcategories of xenobiotics at each respective sampling event. For better comparison y-axis for all bar charts depicts percent of total xenobiotics at the location exhibiting the highest value (a).

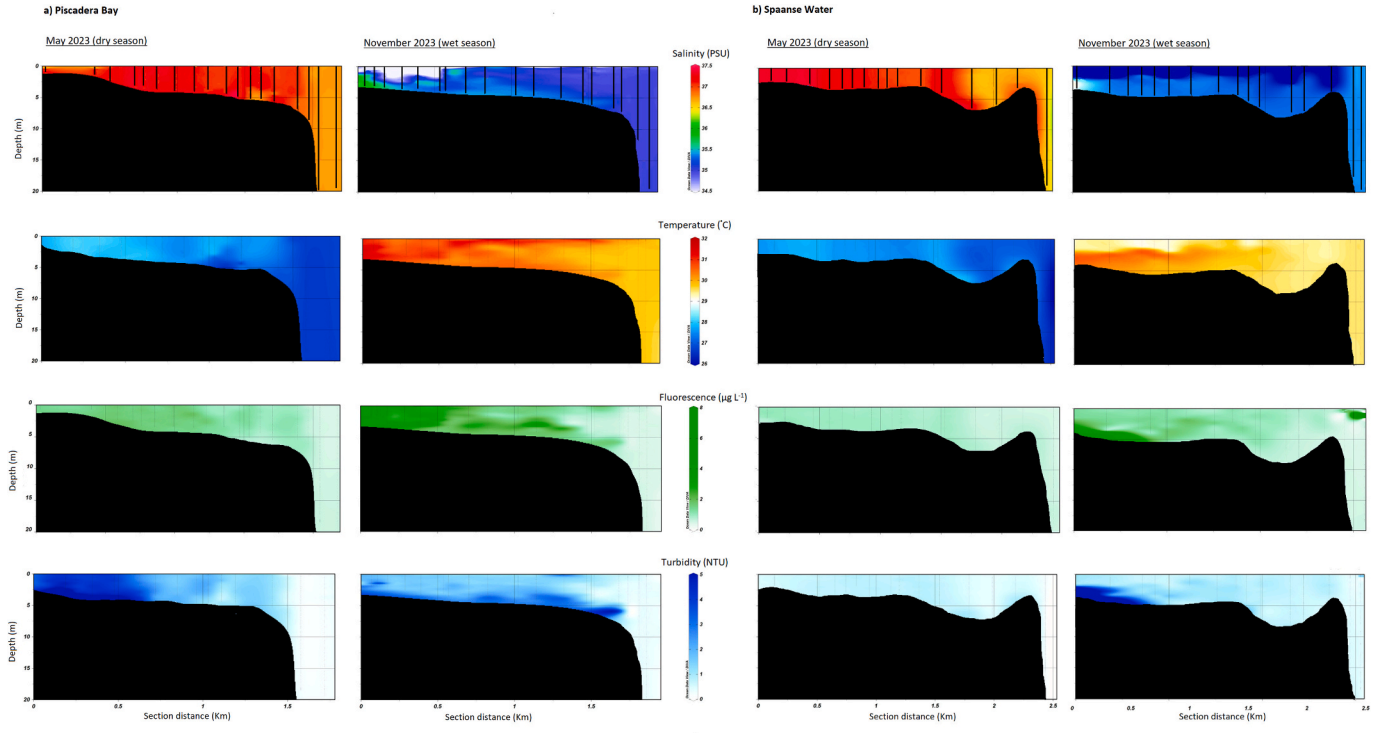

Fig. 5. Water column characteristics of a) Piscadera Bay and b) Spaanse Water in May 2023 (dry season) and November 2023 (wet season). From top to bottom, panels show Salinity, Temperature (°C), Fluorescence (µg L^{-1}) and Turbidity. Black vertical lines in the salinity panels show the 18 and 16 vertical CTD profiles of Piscadera Bay and Spaanse Water respectively. Note that ranges of environmental parameters are different than in Fig. 2 due to El Niño event causing extreme values in 2023.

during the wet season (0.45–0.7 µmol L^{-1}) compared to the dry season (0.2–0.3 µmol L−1; p-values <0.05). Towards the ocean, these values diluted and become similar at a distance of approximately 100–150 m from the bay mouth for both seasons (DIC: 1980–2120 µmol L^{-1}; Si: 1–4 µmol L^{-1}; PO_4: 0.05–0.2 µmol L^{-1}). Similar as in November 2021, higher values of DIC, PO_4 and Si coincide with lower salinity and higher temperature of the bay water. On average, NO_{2+3} and NH_4 measured in the bay were higher in May, also towards the ocean (Fig. 6.a). Most of the highest concentrations measured in May were in the center of the bay.

In Spaanse Water, the water column of the bay in November was charachterized by higher Si, NH_4, NO_{2+3} and DIC values (9–10 µmol L^{-1}; 1.4–1.45 µmol L^{-1}; 0.5–0.7 µmol L^{-1} and 2100–2200 µmol L^{-1}, respectively; Fig. 6.b), particularly in the top layer (1 m below the surface) compared to May (5–6 µmol L^{-1}; 0.4–0.6 µmol L^{-1}; 0.2–0.3 and

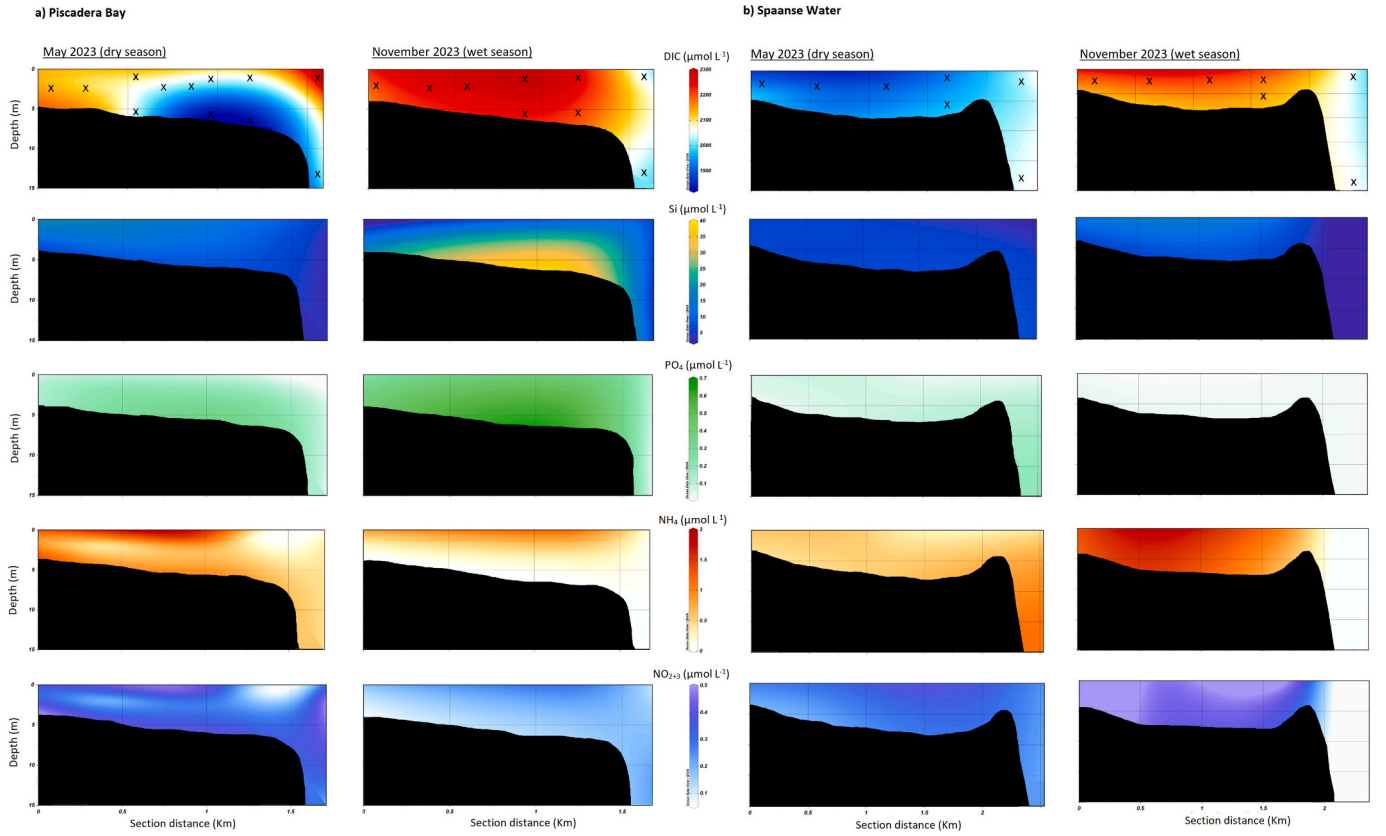

Fig. 6. Inorganic nutrient concentrations measured along a) Piscadera Bay and b) Spaanse Water during May and November 2023. Panels show DIC (µmol L^{-1}), Si (µmol L^{-1}), PO_4 (µmol L^{-1}), NH_4 (µmol L^{-1}) and NO_{2+3} (µmol L^{-1}). Black X in the DIC panels show the depths where water samples were taken. Note that ranges of nutrients are different than in Fig. 3 due to El Niño event causing extreme values in 2023.

2050–2100 µmol L^{-1} respectively; Fig. 6.b). However, NH_4, NO_2 and DIC concentrations towards the open ocean became higher in the dry season. In contrast to Piscadera Bay, PO_4 concentrations were relatively low along the whole transect in both seasons (Fig. 6.b).

3.3. Nutrient export estimations in Piscadera Bay

Using the composition of the bays' waters, we estimated the export of nutrients from Piscadera Bay into the open ocean for the different seasons (Table 1). The nutrient transport data from Piscadera Bay show variations across seasons and years. In November 2021 (wet season), nutrient exports were lower, with silicate ranging from 120 µmol S^{-1} L^{-1} (average speed) to 448.69 µmol S^{-1} L^{-1} (maximum speed), while phosphate showed negative values, indicating potential uptake rather than export. This could be attributed to biological processes such as uptake by phytoplankton, supported by relatively high fluorescence values (3–4 µg L^{-1} in the bay) observed during this period. In May 2022, the dry season exports were higher, with Si transport reaching 364.64 µmol S^{-1} L^{-1} (maximum speed) and positive exports of phosphate and ammonia at 8.60 µmol S^{-1} L^{-1} and 20.64 µmol S^{-1} L^{-1}, respectively. In May 2023 (dry season), average and maximum Si exports increased to 215.51 and 805.82 µmol S^{-1} L^{-1} respectively, with moderate PO_4 and NH_4 exports. The November 2023 wet season shows an increase in nutrient exports, with maximum values reaching 2065.72 µmol S^{-1} L^{-1} for Si, 40.42 µmol S^{-1} L^{-1} for PO_4, and 6.88 µmol S^{-1} L^{-1} for NH_4. DIC export varied widely, with values reaching up to 15,103.68 µmol S^{-1} L^{-1} in November 2023.

Table 1
Estimates of nutrient transports for Piscadera Bay (µmol S^{-1} L^{-1}) (Kamjunke et al., 2023; Wang et al., 2022). Current speed used were the maximum (0.086 (ms^{-1}) and average values (0.023 (ms^{-1})) recorded with an ADCP at 3 m above the seafloor of the bay mouth for 5 days in May 2023.

		Nutrient Transport (µmol S^{-1} L^{-1})				
Date	Water speed	Si	PO_4	NH_4	NO_{2+3}	DIC
Nov-21	Average	120.00	−3.45	0	5.98	427.80
Nov-21	Maximum	448.69	−12.90	0	22.36	1599.60
May-22	Average	97.52	2.30	5.52	0.46	728.19
May-22	Maximum	364.64	8.60	20.64	1.72	2722.83
May-23	Average	215.51	0.92	4.60	0	389.68
May-23	Maximum	805.82	3.44	17.20	0	1457.05
Nov-23	Average	552.46	10.81	1.84	2.3	4039.36
Nov-23	Maximum	2065.72	40.42	6.88	8.60	15,103.68

3.4. Stable isotopes of suspended particulate organic matter in bays

Stable carbon and nitrogen isotope ratios measured along the transects align with patterns in the concentrations of the inorganic nutrients. Significant differences in the isotopic composition were found in both bays during the wet and dry season (Fig. 7, ellipses show grouping with 95 % confidence). In Piscadera Bay (Fig. 7.a), suspended particulate organic matter was more enriched in $\delta^{15}N$ (6.25–12.5 ‰) and less negative in $\delta^{13}C$ (−22 to −18.5 ‰) during the wet seasons compared to the dry seasons (2–6 ‰ and − 27.5 to −22 ‰, respectively). Bay samples collected in the dry season of 2022 showed enriched $\delta^{15}N$ and $\delta^{13}C$ compared to the rest of the dry season samples. More enriched $\delta^{15}N$ values were found in Spaanse Water during the wet season although $\delta^{13}C$ values were similar for both seasons (Fig. 7.b). $\delta^{15}N$ measured during the wet season in the ocean was 1–2 ‰ depleted compared to the bay and the mouth. Overall, waters in Piscadera Bay were more enriched compared to Spaanse Water in $\delta^{15}N$ in both seasons and depleted in $\delta^{13}C$ (2–5 ‰) during the dry season.

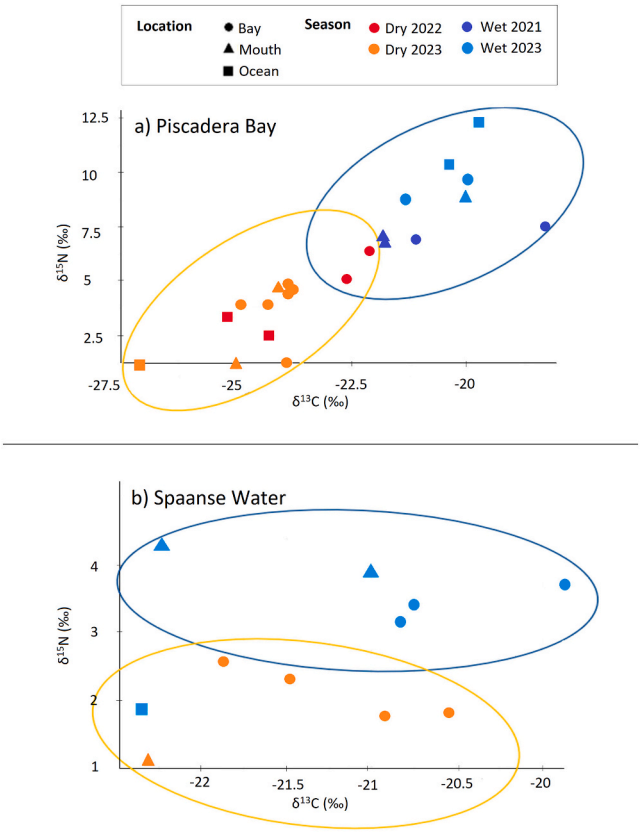

Fig. 7. $\delta^{13}C$ and $\delta^{15}N$ (‰) values measured within a) Piscadera Bay during the dry and wet season of 2021, 2022 and 2023 and b) Spaanse Water during the dry and wet season of 2023. Colors indicate the different seasons and shape where the samples were collected along the transect. Yellow ellipses clusters data of the dry season and blue ellipses of the wet seasons with 95 % confidence.

3.5. Overall chemical variability and relation to environmental parameters

PCA analysis on all seawater chemical data (nutrients, DIC) of Piscadera Bay in 2021–2022 (S3 and S4) showed that most of the variability in the samples relates to the season (i.e. dry versus wet) in which they were taken (Fig. 8.a). Most of the environmental parameters (salinity, temperature, turbidity, distance to bay mouth), however, did not clearly correlate to the seasonal distinction (i.e. they correlate to the first principal component, while the dry and wet seasons align more with the secondary PC axis). Correlations with environmental parameters were positive for 'location' within the transect (i.e. inner bay, mouth or open ocean; 0.93) and depth (0.6) compared to the negative loadings of fluorescence (−0.72) and temperature (−0.39).

Data from Piscadera Bay from 2023 (Fig. 8.b; S3 and S4) clearly differed between the two seasons, and also indicate a distinction between bay and open ocean conditions. This is particularly apparent for dissolved Si concentrations (0.97), PO_4 (0.96) and DIC (0.91) and all these nutrients correlate positively with temperature (0.98), fluorescence (0.72), rainfall (0.95), tide and wind speed (0.95 and 0.96 respectively).

For Spaanse Water (S3 and S4), the result of the principal component analysis is similar to that of Piscadera Bay, showing differences between samples taken in the dry and wet season, as well as those from the open ocean. Samples taken in the wet season are clearly distinguishable, irrespective of their depth or exact location within the bay, from those obtained in the dry season (Fig. 8.c). Samples from the wet season correlate to higher temperatures and more rainfall, whereas variability within the open ocean samples is well correlated to wind speed. Locations within the transect and depth were positively correlated (0.95 and 0.44, respectively) while fluorescence showed a moderately negative correlation (−0.67). These results show that the wet season is influenced by increased precipitation and waters are warmer and have higher fluorescence.

Cluster analysis showed a grouping of the data that was similar for Piscadera Bay and Spaanse Water. In 2021–2022 biochemical data of Piscadera bay clearly clusters by season with water biochemistry in the dry season that is mainly characterized by high DIC, Si and PO_4 concentrations at the deeper part of the inner bay. The wet season on the other hand, was characterized by high Si, NO_2 and NO_3, coinciding with higher rainfall and warmer water. Data of Piscadera Bay collected in 2023 showed similar clusters and correlations as the previous years with the addition of a third cluster containing the open ocean water samples collected during the wet and the dry season that were characterized by lower nutrient concentrations of DIC, Si, PO_4 and NH_4 compared to the bay samples collected in both seasons, showing a positive correlation with wind speed and low rainfall. Finally, the data from Spaanse Water showed the same 3 groups as Piscadera Bay (i.e. bay and mouth samples of the wet season, bay and mouth samples of the dry season and open ocean samples of the dry and wet season).

4. Discussion

We investigated the ocean-bay exchange in two bays with different land-use characteristics and catchment areas along the south coast of Curaçao to determine the role of bays in the distribution of land-derived substances into nearby coastal areas including reef environments. In both bays, a vertical front near the bays' mouths was observed during the dry season, limiting exchange with the open ocean waters. During the wet season, water from the bays and the ocean were mixing more, resulting in higher nutrient fluxes from the bays to the open ocean. In Piscadera Bay the relatively heavy rainfall due to EL Niño-influenced conditions in 2023 resulting in almost four times higher nutrient concentrations in the bays in the wet season and two times higher concentrations in the dry season compared to 2021–2022.

4.1. Seasonal dynamics

Although both bays showed similar trends in the intra-annual environmental characteristics of the water column, average nutrient concentrations varied between years. In May 2022, lower rainfall (1 mm/month compared to the decadal average of 10.2 mm/month for this month (Curaçao Weather, n.d.)) and higher air temperatures than average (+1 °C) likely increased evaporation rates (Sumner and Belaineh, 2005). This corresponds to the relatively high salinities found, particularly at the shallow end of the bay (Fig. 2). Other bays, such as Florida Bay and Chetumal Bay, also showed increased temperatures and salinity due to limited precipitation, with bay-ocean exchange primarily driven by tides and wind forcing (Carrillo et al., 2009; Kelble et al., 2007). Tides are known to affect water exchange, nutrient transport, and mixing dynamics in coastal environments, likely modulating the concentrations of dissolved and particulate substances observed during sampling (Carrillo et al., 2009). In this study, sampling times were not specifically aligned with the tidal cycle, which may have introduced variability in the measured physical and chemical parameters due to tidal influences. However, our results indicate that the highest nutrient concentrations were observed during spring tide in the wet season (Fig. 8), suggesting that tidal dynamics enhance nutrient transport during this period.

In this study the difference in high salinity and temperature between the bay and the open ocean form an ocean front with a barrier effect, which limits the transfer of materials from the bay to the open ocean (Fig. 3). In addition, the observed seasonal variability in Si concentrations, with highest values consistently found in the bay, likely reflects

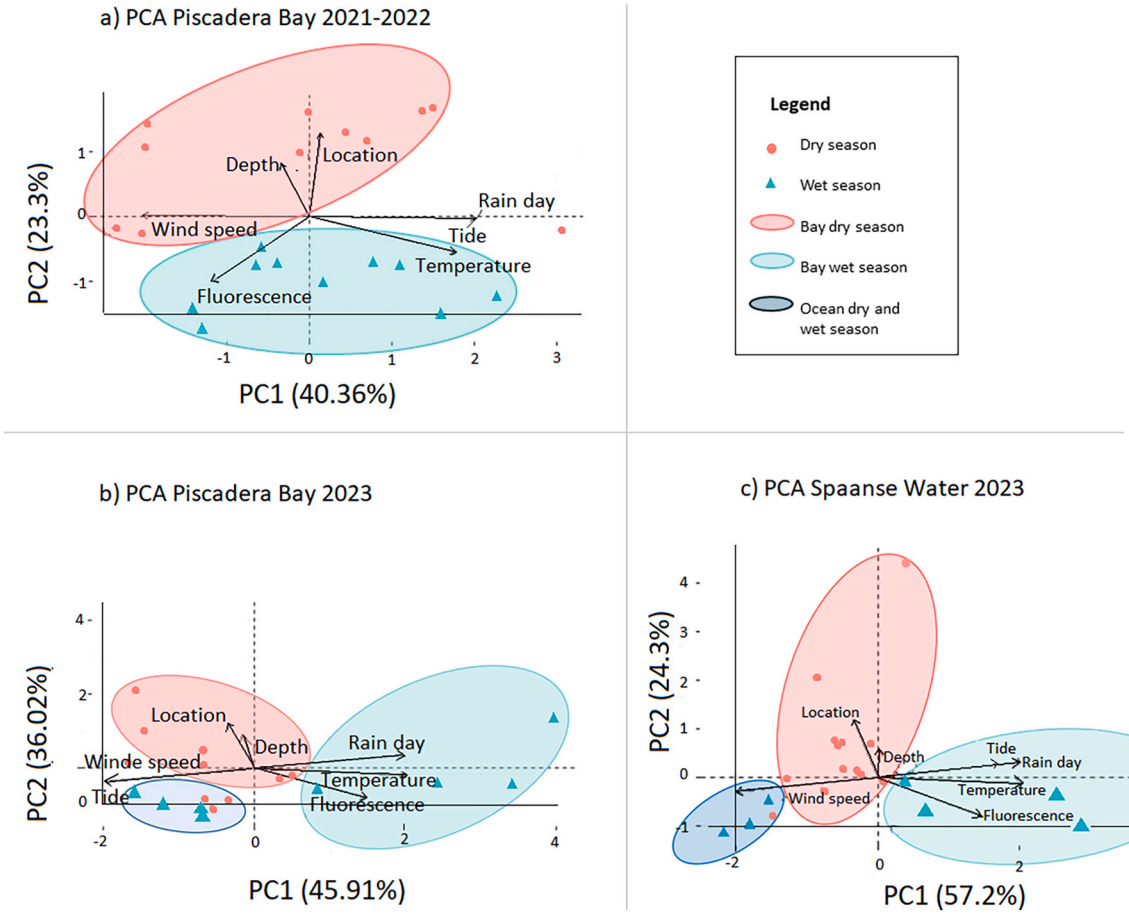

Fig. 8. Principal Component Analysis biplot of a) Piscadera Bay 2021–2022: PC1 accounted for 44.4 % of the total variance with moderate positive loadings of Si (0.73), PO_4 (0.74), NH_4 (0.7) and DIC (0.67) and PC2 accounted for 23.3 % of the total variance with moderate positive loadings of inorganic nutrients of NO_3 (0.66) and DIC (0.64) and negative ones for NO_2 (0.7); b) Piscadera Bay 2023: PC1 explained 45.01 % of the total variance, presenting strong positive loadings of Si (0.97), PO_4 (96) and DIC (91) and PC2 accounted for 36.02 % of the total variance, with strong and moderate positive loading for NH_4, NO_2 and NO_3 (0.96, 0.87, 0.66 respectively) and c) Spaanse Water: PC1 explained 40.36 % result of the strong positive loadings of Si (0.92), NH_4 (0.9), NO_3 (0.79) and DIC (0.78) and PC2 accounted for 23.3 % of the total variance with strong positive loading of PO_4 (0.94) and moderate loading of NO_2 (0.7). Data is colored and shaped by dry (red) and wet (blue) season and black arrows show the environmental variables that have a high contribution to the total variance of the biochemical composition of the water. Ellipses show three cluster groups with a 95 % confidence interval: red for bay and mouth samples in the dry season, light blue for bay and mouth samples in the wet season and dark blue for ocean samples in the dry and wet season. (For interpretation of the references to colour in this figure legend, the reader is referred to the web version of this article.)

natural processes such as water column mixing and terrestrial input from silicate weathering, rather than human activities. This is in contrast to nutrients like nitrogen, which are more strongly influenced by anthropogenic sources (Conley, 2002; Dugdale and Wilkerson, 1998). In 2021–2022, during a moderate La Niña event, lower rainfall in November (77 mm/month compared to the ten year November average of 108 mm/month (Curaçao Weather, n.d.)) likely resulted in reduced surface runoff or input from small streams, leading to less input of inorganic nutrients into Piscadera Bay, as the area lacks large rivers.

Reduced water exchange between bays and the surrounding oceans has been reported for other bays in the western Caribbean (e.g. Chetumal Bay) and in other regions such as the North Atlantic (e.g. Hudson Strait, northern Hudson Bay and southern Foxe Basin) and Indian ocean (e.g. Bay of Bengal) during seasons with limited rainfall (Carrillo et al., 2009; Drinkwater and Jones, 1987; Largier, 2020; Sarma et al., 2016) (Carrillo et al., 2009; Drinkwater and Jones, 1987; Largier, 2020; Sarma et al., 2016).

The exchange between bay and coastal waters also explains the observed levels of anthropogenic pollutants in Piscadera Bay. During the dry season xenobiotic contamination was equally distributed throughout the entire bay with a sharp decrease at the mouth of the bay indicating limited spillover onto the proximate reef systems (Fig. 4). These patterns changed visibly during the wet season where anthropogenic pollution was highest at the landward end of the bay where the sewage outlet is situated. A gradual decrease was observed towards the mouth of the bay, accompanied by a marked spillover into the surrounding coastal waters (Fig. 4). The average concentration of xenobiotics was >1.5 times higher in the wet compared to the dry season, reflecting the increased input of human substances through runoff and sewage. These patterns were visible in almost all subcategories of xenobiotics whereby the highest amount of pollutants was directly attributed to human presence (i.e., human metabolites, substances associated with indoor living spaces, surfactants, and pharmaceuticals). Interestingly, two categories (food contact chemicals and personal care products) showed different patterns with equal or higher abundance in the dry than during wet season. These substances do not necessarily need to be transported into the bay by runoff or discharge but could be introduced directly via the surrounding restaurants, food packaging left on the beach or dumped from boats, and exposure to humans during recreational activities (e.g., swimming, boating, jet ski) (Häder et al., 2020).

In 2023, similar seasonal dynamics were observed in both Piscadera Bay and Spaanse Water, where a front developed during the dry season limiting bay-ocean exchange. This was not the case during the wet

season (Fig. 6), where heavier rainfall in November (129 mm/month compared to the long-term monthly average of 108 mm/month) resulted in almost four times higher nutrient concentrations in the wet season compared to the dry season, when the monthly average rainfall was 4 mm/month (Curaçao Weather, n.d.). Our findings show that nutrient concentrations and fluorescence vary seasonally and interannually. In November 2021 (wet season), chlorophyll *a*utofluorescence and nutrients (e.g., nitrogen) were lower in the bay compared to the open ocean and overall lower than in the dry season of May 2022, when fluorescence and nutrients were higher in the bay than in the open ocean. This suggests an accumulation of nutrients and associated productivity within the bay during the dry season of 2022, potentially due to limited exchange with oceanic waters (Behrenfeld et al., 2009; Cullen, 1982). In contrast, in November 2023 (wet season, El Niño), both fluorescence and nutrients (e.g., DIC, Si, and PO_4) were notably higher in the bay compared to the open ocean and were also significantly higher than during the dry season. This aligns with the higher nutrient export from the bay during the wet season in 2023, driven by rainfall and runoff as well as possibly increased sewage inflow and reduced oceanic flushing. These contrasting observations suggest that the relationship between fluorescence and nutrients varies based on seasonal and interannual factors such as rainfall, nutrient inputs, and exchange between the bay and the ocean. Ultimately, the elevated nutrient concentrations observed during periods of limited water exchange and increased terrestrial inputs could stimulate primary production within the bay, leading to higher chlorophyll-a concentrations. This underscores the role of the bay as a localized hotspot for nutrient accumulation and subsequent phytoplankton growth, with significant implications for bay productivity and ecological dynamics.

In Curaçao most substance input into the bays results from drainage of pipelines or rainfall and subsequent runoff, which is typically associated with pulses of transported material during the wet season (D'Croz et al., 2005; Den Haan et al., 2016). Both of these types of export into the bays were also observed in Spaanse Water although less pronounced than in Piscadera Bay. This may be due to the larger surface area of Spaanse Water, differences in land-use around the two bays, population density or a combination of all.

4.2. Nutrient export

Nutrient export estimations indicate that Piscadera Bay contributes substantial amounts of Si and DIC to the surrounding coastal area, influenced by weather conditions (e.g., rainfall and runoff) and the bay's size and morphology. During the dry season, a thermohaline front forms at the bay mouth due to temperature and salinity differences between the bay and the ocean (Figs. 2 and 5). This front restricts surface mixing and confines water exchange to the bottom layers, causing substances to accumulate in the bay. This period coincides with peak tourist activity (Thielman, 2013). With the onset of the rainy season, increased freshwater inflow enhances surface mixing and bay-ocean exchange, facilitating the discharge of accumulated nutrients and other substances into coastal waters. Similar patterns have been observed in other regions, such as Florida Bay, where nutrient exports are highest during the rainy season (Sutula et al., 2003).

Substances discharged from Curaçao's south coast bays are transported northwest by prevailing surface currents (Bertoncelj et al., 2024; Hernández-Guerra and Joyce, 2000) and likely accumulate in areas of reduced current velocity on the island's west side. These regions have experienced significant coral cover loss in recent decades (Jackson et al., 2014). The seasonal nutrient and pollutant pulses during the dry-to-wet season transition (Fig. 9) present significant challenges for adjacent coral reef ecosystems. Rain-driven inputs of turbid, nutrient-rich water have been linked to coral disease outbreaks (Haapkylä et al., 2011), while elevated concentrations of xenobiotics foster antibiotic-resistant microbial populations, endangering reef communities and human health (Zhang et al., 2022). Warmer, nutrient-enriched waters released during the wet season may further exacerbate reef mortality through increased disease prevalence (Morrow et al., 2011; Quéré et al., 2015).

Residence time plays a critical role in the physical and biogeochemical processes within bays and is known to affect pressure by e.g. eutrophication (Zhao et al., 2022). Although we did not explicitly measure residence times for Piscadera Bay and Spaanse Water, we speculate on the relative changes in residence times by comparing results from the two seasons. During the dry season (May), the development of a pronounced thermohaline front likely increases residence time, as evidenced by the elevated nutrient concentrations (e.g., NH_4 and DIC) in the bay relative to the ocean. In contrast, during the wet season higher rainfall and increased runoff will lower the salinity, equilibrating the conditions inside and outside the bay. This will result in increased mixing during the wet season (November) and reduce residence time as shown by the more homogeneous water column profiles of temperature and salinity and smaller difference in water geochemistry within and outside the bay. Nutrient transport data for Piscadera Bay (Table 1) supports this interpretation, with higher nutrient export values in November 2023 indicative of increased water exchange and lower residence times, while lower export values in May 2023 suggest reduced exchange and likely longer residence times.

Smaller temperature and salinity differences between Spaanse Water and the open ocean suggest that Spaanse Water houses water with a shorter residence time. This is likely related to differences in bay

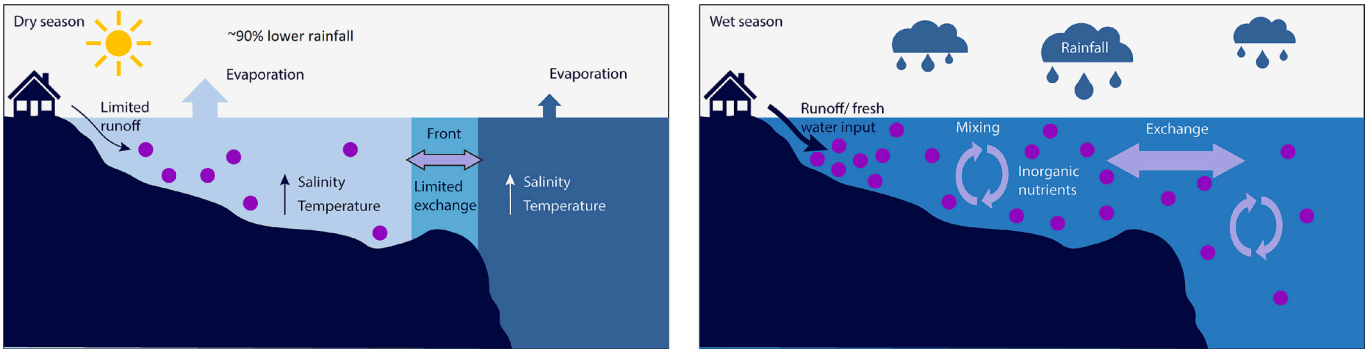

Fig. 9. Left pannel shows a schematic representation of the main processes affecting bay-ocean exchange during the dry season. Low runoff input, ~90 % lower rainfall compared to the wet season and high air temperatures result in higher eveporation in the bay compared to the open ocean. Temperature and salinity difference between the bay and the ocean lead to the development of a front at the mouth that limits the bay-ocean exchange. Nutrient concentrations (represented by purple dots) are higher in the bay compared to the open ocean Right pannel shows how higher run-off and rainfall during the wet season result in more mixing and the dissapearance of the front, allowing more exchange with the open ocean. (For interpretation of the references to colour in this figure legend, the reader is referred to the web version of this article.)

morphology, volume of water and water exchange dynamics at the bay mouth. Water exchange within bays plays a critical role in determining how bays respond to pollutant inputs, including nutrients. As this study shows, restricted water exchange can lead to prolonged residence times, promoting the accumulation of nutrients and enhancing eutrophication risks. Conversely, increased exchange with offshore waters, as observed during the wet season when stratification is reduced, can dilute nutrient concentrations, mitigating their impacts. The local hydrodynamics of bays, including the effect of tides will thus directly affect the transport and fate of pollutants, as well as their subsequent influence on nearby ecosystems. Future studies employing hydrodynamic models or tracer experiments are essential to accurately estimate residence times, offering valuable insights into nutrient dynamics and their links to eutrophication.

4.3. Bays and coral reefs

The transition periods between the dry and wet season, when bays change their role from a net sink of land-derived matter to a source can influence the health state of nearby coral reefs. Reefs along the south coast of Curaçao have lost >50 % of coral cover in the last 50 years (Jacobs, 2022; Sandin et al., 2022), resembling the global trend of coral reef decline as a result of increased human pressure. On a smaller scale, the exact decline (or even absence thereof) can be modulated by variability in the organic matter input, sedimentation and thermal stress caused by nearby bays (Weber et al., 2012).

The high concentrations measured for most of the nutrients in Piscadera Bay and Spaanse Water can result in eutrophication. As shown here and by others both bays have been reported to be a substantial point source for human derived substances from coastal residencies, high coastal development and boat activity (Govers et al., 2014; Van Tussenbroek et al., 2016). According to Slijkerman et al. (2014), concentrations higher than ~1 μmol L^{-1} for nitrogen and ~ 0.1 μmol L^{-1} for phosphorous are indicative for eutrophied waters. The concentration of phosphorus, nitrogen and silicate measured in both bays exceeded these eutrophication threshold values during the dry and wet season, being significantly higher during the wet season of 2023. While symptoms of eutrophication, such as increased algal growth, were not explicitly monitored in this study, the elevated nutrient levels, particularly during the wet season, indicate the potential for eutrophication to occur in these environments. Such concentrations in water overlaying reefs can negatively affect coral growth, calcification and coral reproduction (Vega Thurber et al., 2013). Although there are no studies directly measuring the impact of these bays on nearby coral reefs, Govers et al. (2014) demonstrated that other ecosystems, such as seagrasses, are threatened by eutrophication resulting from emergency wastewater overflow and coastal housing near these two bays. Furthermore, coral populations inside Curaçao's bays have shown significantly lower coral cover and colony density compared to those on nearby fringing reefs, with a greater decline among broadcast-spawning species, likely due to higher post-settlement mortality in the more extreme bay environments (Vermeij et al., 2007).

The $\delta^{15}N$ values of particulate suspended organic matter can be used as a tracer to identify eutrophication (Abreu et al., 2006). Anthropogenic nitrogen input, as shown in this study by enriched inorganic nutrient concentrations and high $\delta^{15}N$ values measured in the bays and open ocean during the wet seasons can have a harmful effect on reef systems (Geeraert et al., 2020). Piscadera Bay showed greater $\delta^{15}N$ enrichment and seasonal $\delta^{13}C$ variation compared to Spaanse Water, suggesting stronger anthropogenic influence and localized biological activity. Differences between the bays likely result from variations in their hydrodynamic regimes, connectivity to the ocean, and catchment area sizes (Largier, 2020). Eutrophication and the high retention time in bays can have crucial ecological implications on nearby reef systems, such as phytoplankton blooms or cyanobacterial, turf and algal growth (Brocke et al., 2015; Largier, 2020). These effects, in turn, may have a synergetic role amplifying climate change effects (Den Haan et al., 2016; Gast et al., 1999). Therefore, it is important to quantify and determine the temporal variability in bay-ocean exchange and its effect on nearby reefs, which is not only governed by the input from land derived substances into the bays, but also by the bay size, the connection to the ocean and by the area from which they collect rainwater (i.e. the size of the surrounding catchment area). Future modelling efforts are needed to predict the tipping point when a bay is from a catchment area into a source area of pollutants. Knowledge on these tipping points is essential for conservation and management plans to reduce the effect on coastal benthic communities.

Isotopic values showed seasonal differences in both bays and indicated more exchange with open ocean seawater at Spaanse Water. Heavier $\delta^{15}N$ measured in Piscadera Bay likely relates to the influence of an emergency overflow pipe in this bay (Govers et al., 2014). The highly depleted $\delta^{13}C$ values, especially in the dry seasons, support the strong land influence affecting this bay and the little exchange with the open ocean (Abreu et al., 2006; Simenstad and Wissmar, 1985). In comparison, Spaanse Water showed much lighter $\delta^{15}N$ values than Piscadera Bay during the wet season, indicating either less land derived input or higher dilution of land derived matter due to the size of the bay or the bigger mouth opening. Furthermore, the relatively heavier $\delta^{13}C$ illustrates a stronger marine influence and therefore increased bay-ocean mixing (Abreu et al., 2006).

4.4. El Niño event: a window to understanding future climate conditions?

November 2023 saw relatively high export rates of substances from within the two studied bays, which may be indicative for the effect of bays as climate changes further. The Caribbean Antilles sea surface temperature has already increased by 1.32 ± 0.41 °C in the last century (Jones et al., 2016; Stephenson et al., 2014) and varies currently between ~26.5 °C in the dry season to maximum temperatures of 28.5 °C in the wet season (McField, 2017). In this study we recorded temperatures of ~30.7 °C in the bays and ~ 29.8 °C in the open ocean close to the bays in November, exceeding historical norms for the region. Moreover, in the dry season, temperatures in the bay exceeded the decadal average temperature of May by ~1.2 °C. The export from these bays may temporarily add to the overall increase in nutrient load and rising temperatures affecting coral reefs. The critical thresholds for tropical coral reefs with temperatures of 21.7–29.6 °C, salinities of 28.7–40.4, nitrate and phosphate concentrations of 4.51 and 0.63 μmol L^{-1}, respectively (Berkelmans et al., 2012; Guan et al., 2015), maybe seasonally crossed in areas influenced by bay export.

Benthic communities in in these bays, such as corals in Piscadera Bay and seagrass beds in Spaanse Water, have historically experienced declines attributed to urban development and pollution(Debrot et al., 1998; Nagelkerken et al., 2005). Although some of the benthic cover loss has also been related to bleaching events (Debrot et al., 1998), studies have shown that high turbidity in tropical bays result in higher coral resilience of prolongated elevated sea temperatures and therefore reduce coral bleaching (Morgan et al., 2017; Schoepf et al., 2023; Sully and van Woesik, 2020; Zweifler et al., 2021). In addition, hard corals living in extreme environment such as intertidal areas where they are exposed to high and variable water temperatures can develop heat tolerance (Barshis et al., 2013; Schoepf et al., 2020). Understanding how these benthic ecosystems adapt to such extremes is critical for predicting their responses to future global warming scenarios and informing conservation strategies.

Overall, this study highlights that extreme events, such as the 2023 El Niño, can amplify nutrient and pollutant export from bays into coastal environments. However, given the limited dataset encompassing one El Niño and one La Niña event, further long-term studies are needed to confirm these patterns and assess their broader implications.

5. Conclusions

This study shows that bay-ocean exchange in Curaçao is higher during the wet season than in the dry season. Water properties, such as temperature, salinity, turbidity, and concentrations of inorganic nutrients, Si, DIC, and SPM, vary significantly between the bays and adjacent open ocean areas. During the dry season, the bays accumulate substances, which are then periodically released during the wet season, increasing the nutrient, suspended matter and pollutant load in the shallow reef ecosystems. These variations in chemical fluxes between the bays and coastal waters reflect differences in nutrient and pollutant transport, with enhanced exports during the wet season driven by surface runoff and higher rainfall. Extreme events, such as the 2023 El Niño, amplified the export of substances from these bays into nearby reefs. The presence of anthropogenic substances, such as pharmaceuticals, personal care products, and pesticides, also contributes to the chemical composition of the bay and coastal waters, being also higher during the wet season. As El Niño events are expected to become more frequent these extreme conditions measured in bays in Curaçao may be representative for future climate scenarios and could be used to understand how reefs may react to these predicted environmental changes. Quantifying and characterizing the suspended matter and pollutants released from the bays, and understanding their potential impacts on reef health, are crucial for assessing how these bays contribute to reef degradation and for developing effective conservation measures and management strategies.

CRediT authorship contribution statement

V. Sanchez Barranco: Writing – original draft, Visualization, Methodology, Investigation, Formal analysis, Data curation, Conceptualization. **L. Schellenberg:** Writing – review & editing, Visualization, Methodology, Investigation, Formal analysis. **F. Mienis:** Writing – review & editing, Supervision, Project administration, Investigation, Funding acquisition, Conceptualization. **C.P.D. Brussaard:** Writing – review & editing, Supervision, Conceptualization. **A.F. Haas:** Writing – review & editing, Supervision, Conceptualization. **L.J. de Nooijer:** Writing – review & editing, Supervision, Project administration, Investigation, Funding acquisition, Conceptualization.

Declaration of competing interest

The authors declare that they have no known competing financial interests or personal relationships that could have appeared to influence the work reported in this paper.

Acknowledgements

This publication is part of the project “Land, Sea, and Society: Linking terrestrial pollutants and inputs to nearshore coral reef growth to identify novel conservation options for the Dutch Caribbean (SEALINK)” with project number NWOCA.2019.003 of the research program “Caribbean Research: a Multidisciplinary Approach” which is (partly) financed by the Dutch Research Council (NWO). We heartly thank the project leader M J A Vermeij for facilitating our work at CARMABI. We thank the PhD students Vesna Bertoncelj, Nienke C J van de Loosdrecht that helped collecting the samples and Titus Kruijssen for providing the data of the catchment areas. We greatly acknowledge the technicians of Ocean Systems and Marine Microbiology and Biogeochemistry department at NIOZ for their hard work and expert abilities. Furthermore, we would like to thank Daniel Petras and the Functional Metabolomics Lab for their expertise regarding the metabolomics-xenobiotics data processing. The Marine Park Rangers and team of CARMABI that helped sampling around the island are also heartly thanked. We greatly acknowledge the hard work of the master students Marina Adler, Tom van Ee and Francine van Hee for their dedication during fieldworks.

Appendix A. Supplementary data

Supplementary data to this article can be found online at https://doi.org/10.1016/j.marpolbul.2025.117545.

Data availability

The data supporting this study are openly available and can be accessed via the DOI: 10.25850/nioz7b.b.0h.

References

Abreu, P.C., Costa, C.S., Bemvenuti, C., Odebrecht, C., Graneli, W., Anesio, A.M., 2006. Eutrophication processes and trophic interactions in a shallow estuary: preliminary results based on stable isotope analysis (δ 13 C and δ 15 N). Estuar. Coasts 29, 277–285.

Adey, W.H., Steneck, R.S., 1985. Highly productive eastern Caribbean reefs: synergistic effects of biological, chemical, physical, and geological factors. The ecology of coral reefs 3, 163–187.

Aydin-Onen, S., Kocak, F., Kucuksezgin, F., 2012. Evaluation of spatial and temporal variations of inorganic nutrient species in the eastern Aegean Sea waters. Mar. Pollut. Bull. 64 (12), 2849–2856.

Barshis, D.J., Ladner, J.T., Oliver, T.A., Seneca, F.O., Traylor-Knowles, N., Palumbi, S.R., 2013. Genomic basis for coral resilience to climate change. Proc. Natl. Acad. Sci. 110 (4), 1387–1392.

Behrenfeld, M.J., Westberry, T.K., Boss, E., O'Malley, R.T., Siegel, D.A., Wiggert, J.D., Franz, B., McClain, C., Feldman, G., Doney, S.C., 2009. Satellite-detected fluorescence reveals global physiology of ocean phytoplankton. Biogeosciences 6 (5), 779–794.

Berkelmans, R., Jones, A., Schaffelke, B., 2012. Salinity thresholds of Acropora spp. on the Great Barrier Reef. Coral Reefs 31, 1103–1110.

Bertoncelj, V., Mienis, F., Stocchi, P., van Sebille, E., 2024. Flow Patterns, Hotspots and Connectivity of Land-Derived Substances at the Sea Surface of Curaçao in the Southern Caribbean. Preprint. EGUsphere. https://doi.org/10.5194/egusphere-2024-3112.

Brocke, H.J., Polerecky, L., De Beer, D., Weber, M., Claudet, J., Nugues, M.M., 2015. Organic matter degradation drives benthic cyanobacterial mat abundance on Caribbean coral reefs. PLoS One 10 (5), e0125445.

Caballero-Gallardo, K., Alcala-Orozco, M., Barraza-Quiroz, D., De la Rosa, J., Olivero-Verbel, J., 2020. Environmental risks associated with trace elements in sediments from Cartagena Bay, an industrialized site at the Caribbean. Chemosphere 242, 125173.

Carrillo, L., Palacios-Hernández, E., Yescas, M., Ramírez-Manguilar, A.M., 2009. Spatial and seasonal patterns of salinity in a large and shallow tropical estuary of the Western Caribbean. Estuaries and Coasts 32, 906–916.

Conley, D.J., 2002. Terrestrial ecosystems and the global biogeochemical silica cycle. Global Biogeochem. Cycles 16 (4), 68-61-68-68.

Cullen, J.J., 1982. The deep chlorophyll maximum: comparing vertical profiles of chlorophyll a. Can. J. Fish. Aquat. Sci. 39 (5), 791–803.

Curaçao Weather. n.d. (Retrieved 5-9-2024 from).

D'Croz, L., Ross Robertson, D., Martínez, J.A., 1999. Cross-shelf distribution of nutrients, plankton, and fish larvae in the San Blas Archipelago, Caribbean Panama. Revista de biología tropical 47 (1–2), 203–215.

D'Croz, L., Rosario, J.B., d., & Gondola, P., 2005. The effect of fresh water runoff on the distribution of dissolved inorganic nutrients and plankton in the Bocas del Toro archipelago, Caribbean Panama. Caribb. J. Sci Vol. 41, No. 3, 414-429.

Debrot, A., Kuenen, M., Dekker, K., 1998. Recent declines in the coral fauna of the Spaanse Water, Curaçao, Netherlands Antilles. Bulletin of Marine Science 63 (3), 571–580.

Den Haan, J., Huisman, J., Brocke, H.J., Goehlich, H., Latijnhouwers, K.R., Van Heeringen, S., Honcoop, S.A., Bleyenberg, T.E., Schouten, S., Cerli, C., 2016. Nitrogen and phosphorus uptake rates of different species from a coral reef community after a nutrient pulse. Sci. Rep. 6 (1), 28821.

Devlin, M., Brodie, J., 2023. Nutrients and eutrophication. In: Marine Pollution–Monitoring, Management and Mitigation. Springer, pp. 75–100.

Dittmar, T., Koch, B., Hertkorn, N., Kattner, G., 2008. A simple and efficient method for the solid-phase extraction of dissolved organic matter (SPE-DOM) from seawater. Limnol. Oceanogr. Methods 6 (6), 230–235.

Drinkwater, K., Jones, E., 1987. Density stratification, nutrient and chlorophyll distributions in the Hudson Strait region during summer and their relation to tidal mixing. Cont. Shelf Res. 7 (6), 599–607.

Dugdale, R.C., Wilkerson, F.P., 1998. Silicate regulation of new production in the equatorial Pacific upwelling. Nature 391 (6664), 270–273.

Fabricius, K.E., 2011. Factors determining the resilience of coral reefs to eutrophication: a review and conceptual model. Coral reefs: an ecosystem in transition 493–505.

Gast, G., Jonkers, P., Van Duyl, F., Bak, R., 1999. Bacteria, flagellates and nutrients in island fringing coral reef waters: influence of the ocean, the reef and eutrophication. Bull. Mar. Sci. 65 (2), 523–538.

Geeraert, N., Duprey, N.N., McIlroy, S.E., Thompson, P.D., Goldstein, B.R., LaRoche, C., Kim, K., Raymundo, L.J., Baker, D.M., 2020. The anthropogenic nitrogen footprint of a tropical lagoon: spatial variability in Padina sp. δ15N values1. Pac. Sci. 74 (1), 19–29.

Gobler, C.J., Cullison, L.A., Koch, F., Harder, T.M., Krause, J.W., 2005. Influence of freshwater flow, ocean exchange, and seasonal cycles on phytoplankton–nutrient dynamics in a temporarily open estuary. Estuar. Coast. Shelf Sci. 65 (1–2), 275–288.
Govers, L.L., Lamers, L.P., Bouma, T.J., de Brouwer, J.H., van Katwijk, M.M., 2014. Eutrophication threatens Caribbean seagrasses–an example from Curaçao and Bonaire. Mar. Pollut. Bull. 89 (1–2), 481–486.
Grasshoff, K., Kremling, K., Ehrhardt, M., 2009. Methods of Seawater Analysis. John Wiley & Sons.
Guan, Y., Hohn, S., Merico, A., 2015. Suitable environmental ranges for potential coral reef habitats in the tropical ocean. PloS One 10 (6), e0128831.
Haapkylä, J., Unsworth, R.K., Flavell, M., Bourne, D.G., Schaffelke, B., Willis, B.L., 2011. Seasonal rainfall and runoff promote coral disease on an inshore reef. PloS One 6 (2), e16893.
Häder, D.-P., Banaszak, A.T., Villafañe, V.E., Narvarte, M.A., González, R.A., Helbling, E. W., 2020. Anthropogenic pollution of aquatic ecosystems: emerging problems with global implications. Sci. Total Environ. 713, 136586.
Hawkes, J.A., Patriarca, C., Sjöberg, P.J., Tranvik, L.J., Bergquist, J., 2018. Extreme isomeric complexity of dissolved organic matter found across aquatic environments. Limnology and Oceanography Letters 3 (2), 21–30.
Hearn, C.J., 2011. Perspectives in coral reef hydrodynamics. Coral Reefs 30 (Suppl. 1), 1–9.
Helder, W., De Vries, R., 1979a. An automatic phenol-hypochlorite method for the determination of ammonia in sea-and brackish waters. Neth. J. Sea Res. 13 (1), 154–160.
Helder, W., De Vries, R.T.P., 1979b. An automatic phenol-hypochlorite method for the determination of ammonia in sea-and brackish waters. Netherlands Journal of Sea Research 13 (1), 154–160.
Hernández-Guerra, A., Joyce, T.M., 2000. Water masses and circulation in the surface layers of the Caribbean at 66 W. Geophys. Res. Lett. 27 (21), 3497–3500.
Hersbach, H., Bell, B., Berrisford, P., Hirahara, S., Horányi, A., Muñoz-Sabater, J., Nicolas, J., Peubey, C., Radu, R., Schepers, D., 2020. The ERA5 global reanalysis. Q. J. Roy. Meteorol. Soc. 146 (730), 1999–2049.
Hydes, D.J., Aoyama, M., Aminot, A., Bakker, K., Becker, S., Coverly, S., Daniel, A., Dickson, A.G., Grosso, O., Kerouel, R., van Ooijen, J., Sato, K., Tanhua, T., Woodward, E.M.S., Zhang, J.Z., 2010. Determination of Dissolved Nutrients (N, P, Si) in Seawater with High Precision and Inter-Comparability Using Gas-Segmented Continuous Flow Analysers.
Jackson, J., Donovan, M., Cramer, K., Lam, V., 2014. Status and Trends of Caribbean Coral Reefs: 1970–2012. Global Coral Reef Monitoring Network; International …, Gland, Switzerland.
Jacobs, R., 2022. Numerical Simulation of Submarine Groundwater Discharge: A Case Study in Curaçao.
Johnston, E.L., Roberts, D.A., 2009. Contaminants reduce the richness and evenness of marine communities: a review and meta-analysis. Environ. Pollut. 157 (6), 1745–1752.
Jones, P.D., Harpham, C., Harris, I., Goodess, C.M., Burton, A., Centella-Artola, A., Taylor, M.A., Bezanilla-Morlot, A., Campbell, J.D., Stephenson, T.S., 2016. Long-term trends in precipitation and temperature across the Caribbean. Int. J. Climatol. 36 (9), 3314–3333.
Kamjunke, N., Brix, H., Flöser, G., Bussmann, I., Schütze, C., Achterberg, E.P., Ködel, U., Fischer, P., Rewrie, L., Sanders, T., 2023. Large-scale nutrient and carbon dynamics along the river-estuary-ocean continuum. Sci. Total Environ. 890, 164421.
Kelble, C.R., Johns, E.M., Nuttle, W.K., Lee, T.N., Smith, R.H., Ortner, P.B., 2007. Salinity patterns of Florida Bay. Estuar. Coast. Shelf Sci. 71 (1–2), 318–334.
Kennish, M.J., 2009. Eutrophication of mid-Atlantic coastal bays. Bull. NJ Acad. Sci 54 (3), 1–8.
Kjerfve, B., Magill, K.E., 1989. Geographic and hydrodynamic characteristics of shallow coastal lagoons. Mar. Geol. 88 (3–4), 187–199.
Lao, Q., Zhang, S., Li, Z., Chen, F., Zhou, X., Jin, G., Huang, P., Deng, Z., Chen, C., Zhu, Q., 2022. Quantification of the seasonal intrusion of water masses and their impact on nutrients in the Beibu Gulf using dual water isotopes. J. Geophys. Res. Oceans 127 (7), e2021JC018065.
Lapointe, B., Thacker, K., Hanson, C., Getten, L., 2011. Sewage pollution in Negril, Jamaica: effects on nutrition and ecology of coral reef macroalgae. Chinese J. Oceanol. Limnol. 29, 775–789.
Largier, J.L., 2020. Upwelling bays: how coastal upwelling controls circulation, habitat, and productivity in bays. Ann. Rev. Mar. Sci. 12, 415–447.
Martis, A., van Oldenborgh, G.J., Burgers, G., 2001. Predicting Rainfall in the Dutch Caribbean—More than El Niño? Koninklijk Nederlands Meteorologisch Instituut.
McField, M., 2017. Impacts of climate change on coral in the coastal and marine environments of Caribbean Small Island Developing States (SIDS). Caribbean marine climate change report card: Science Review 2017, 52–59.
Mestres, M., Sanchéz-Arcilla, A., Sierra, J.P., Mösso, C., Tagliani, P., Möller, O., Niencheski, L., 2006. Coastal bays as a sink for pollutants and sediment. J. Coast. Res. 1546–1550.
Mohammed Taha, H., Aalizadeh, R., Alygizakis, N., Antignac, J.-P., Arp, H.P.H., Bade, R., Baker, N., Belova, L., Bijlsma, L., Bolton, E.E., 2022. The NORMAN Suspect List Exchange (NORMAN-SLE): facilitating European and worldwide collaboration on suspect screening in high resolution mass spectrometry. Environ. Sci. Eur. 34 (1), 104.
Morgan, K.M., Perry, C.T., Johnson, J.A., Smithers, S.G., 2017. Nearshore turbid-zone corals exhibit high bleaching tolerance on the Great Barrier Reef following the 2016 ocean warming event. Front. Mar. Sci. 4, 224.
Morrow, K., Paul, V.J., Liles, M., Chadwick, N., 2011. Allelochemicals produced by Caribbean macroalgae and cyanobacteria have species-specific effects on reef coral microorganisms. Coral Reefs 30, 309–320.
Murphy, J., Riley, J.P., 1962. A modified single solution method for the determination of phosphate in natural waters. Anal. Chim. Acta 27, 31–36.
Nagelkerken, I., Vermonden, K., Moraes, O., Debrot, A., Nagelkerken, W., 2005. Changes in coral reef communities and an associated reef fish species, Cephalopholis cruentata (Lacepede), after 30 years on Curacao (Netherlands Antilles). Hydrobiologia 549, 145–154.
Nothias, L.-F., Petras, D., Schmid, R., Dührkop, K., Rainer, J., Sarvepalli, A., Protsyuk, I., Ernst, M., Tsugawa, H., Fleischauer, M., 2020. Feature-based molecular networking in the GNPS analysis environment. Nat. Methods 17 (9), 905–908.
Odum, E.P., 1980. The status of three ecosystem-level hypotheses regarding salt marsh estuaries: Tidal subsidy, outwelling, and detritus-based food chains. In: Estuarine perspectives. Elsevier, pp. 485–495.
Pakkir Shah, Walter, A., Ottosson, F., Russo, F., Navarro-Diaz, M., Boldt, J., Petras, D., 2024. Statistical analysis of feature-based molecular networking results from non-targeted metabolomics data. Nature protocols,, 1–71.
Petras, D., Koester, I., Da Silva, R., Stephens, B.M., Haas, A.F., Nelson, C.E., Kelly, L.W., Aluwihare, L.I., Dorrestein, P.C., 2017. High-resolution liquid chromatography tandem mass spectrometry enables large scale molecular characterization of dissolved organic matter. Front. Mar. Sci. 4, 405.
Piwowarska, D., Kiedrzyńska, E., 2022. Xenobiotics as a contemporary threat to surface waters. Ecohydrology and Hydrobiology 22 (2), 337–354.
Quéré, G., Meistertzheim, A.-L., Steneck, R.S., Nugues, M.M., 2015. Histopathology of crustose coralline algae affected by white band and white patch diseases. PeerJ 3, e1034.
van Sambeek, M.H., Eggenkamp, H.G.M., Vissers, M., 2000. The groundwater quality of Aruba, Bonaire and Curaçao: a hydrogeochemical study. Neth. J. Geosci. 79 (4), 459–466.
Sandin, S.A., Alcantar, E., Clark, R., de León, R., Dilrosun, F., Edwards, C.B., Estep, A.J., Eynaud, Y., French, B.J., Fox, M.D., 2022. Benthic assemblages are more predictable than fish assemblages at an island scale. Coral Reefs 41 (4), 1031–1043.
Sarma, V., Rao, G., Viswanadham, R., Sherin, C., Salisbury, J., Omand, M.M., Mahadevan, A., Murty, V., Shroyer, E.L., Baumgartner, M., 2016. Effects of freshwater stratification on nutrients, dissolved oxygen, and phytoplankton in the Bay of Bengal. Oceanography 29 (2), 222–231.
Schlitzer, R., 2012. Ocean Data View, Edited.
Schoepf, V., Jung, M.U., McCulloch, M.T., White, N.E., Stat, M., Thomas, L., 2020. Thermally variable, macrotidal reef habitats promote rapid recovery from mass coral bleaching. Front. Mar. Sci. 7, 245.
Schmid, R., Heuckeroth, S., Korf, A., Smirnov, A., Myers, O., Dyrlund, T.S., Pluskal, T., 2023. Integrative analysis of multimodal mass spectrometry data in MZmine 3. Nature biotechnology 41 (4), 447–449.
Schoepf, V., Baumann, J.H., Barshis, D.J., Browne, N.K., Camp, E.F., Comeau, S., Cornwall, C.E., Guzmán, H.M., Riegl, B., Rodolfo-Metalpa, R., 2023. Corals at the edge of environmental limits: a new conceptual framework to re-define marginal and extreme coral communities. Sci. Total Environ. 163688.
Shrestha, S., Kazama, F., 2007. Assessment of surface water quality using multivariate statistical techniques: a case study of the Fuji river basin, Japan. Environmental Modelling & Software 22 (4), 464–475.
Simenstad, C.A., Wissmar, R.C., 1985. d13C evidence of the origins and fates of organic carbon in estuarine and nearshore food webs. Mar. Ecol. Prog. Ser. 22, 141–152.
Siung-Chang, A., 1997. A review of marine pollution issues in the Caribbean. Environ. Geochem. Health 19 (2), 45–55.
Slijkerman, D.M., de León, R., de Vries, P., 2014. A baseline water quality assessment of the coastal reefs of Bonaire, Southern Caribbean. Marine pollution bulletin 86 (1–2), 523–529.
Stephenson, T.S., Vincent, L.A., Allen, T., Van Meerbeeck, C.J., McLean, N., Peterson, T. C., Taylor, M.A., Aaron-Morrison, A.P., Auguste, T., Bernard, D., 2014. Changes in extreme temperature and precipitation in the Caribbean region, 1961–2010. Int. J. Climatol. 34 (9), 2957–2971.
Steward, R., Chopin, P., Verburg, P.H., 2024. Supporting spatial planning with a novel method based on participatory Bayesian networks: an application in Curaçao. Environ. Sci. Policy 156, 103733.
Stoll, M.H.C., Bakker, K., Nobbe, G.H., Haese, R.R., 2001. Continuous-flow analysis of dissolved inorganic carbon content in seawater. Anal. Chem. 73 (17), 4111–4116.
Strickland, J.D.H., Parsons, T.R., 1972a. A Practical Handbook of Seawater Analysis.
Strickland, J.D.H., Parsons, T.R., 1972b. A Practical Handbook of Seawater Analysis. Fisheries Research Board of Canada, Nr, p. 167.
Sully, S., van Woesik, R., 2020. Turbid reefs moderate coral bleaching under climate-related temperature stress. Glob. Chang. Biol. 26 (3), 1367–1373.
Sumner, D., Belaineh, G., 2005. Evaporation, precipitation, and associated salinity changes at a humid, subtropical estuary. Estuaries 28 (6), 844–855.
Sutula, M.A., Perez, B.C., Reyes, E., Childers, D.L., Davis, S., Day Jr., J.W., Rudnick, D., Sklar, F., 2003. Factors affecting spatial and temporal variability in material exchange between the Southern Everglades wetlands and Florida Bay (USA). Estuar. Coast. Shelf Sci. 57 (5–6), 757–781.
Teece, M.A., Fogel, M.L., 2004. Preparation of ecological and biochemical samples for isotope analysis. In: Handbook of Stable Isotope Analytical Techniques. Elsevier, pp. 177–202.
Thielman, S., 2013. The Effects of Tourism Developments on the Built Environment in Small Island Developing States, Scenarios, Frameworks: The Case Study of Curacao.
Tuholske, C., Halpern, B.S., Blasco, G., Villasenor, J.C., Frazier, M., Caylor, K., 2021. Mapping global inputs and impacts from of human sewage in coastal ecosystems. PloS One 16 (11), e0258898.
Van Tussenbroek, B., Van Katwijk, M., Bouma, T., Van der Heide, T., Govers, L., Leuven, R., 2016. Non-native seagrass Halophila stipulacea forms dense mats under eutrophic conditions in the Caribbean. J. Sea Res. 115, 1–5.

Vega Thurber, Burkepile, D.E., Fuchs, C., Shantz, A.A., McMinds, R., Zaneveld, J.R., 2014. Chronic nutrient enrichment increases prevalence and severity of coral disease and bleaching. Global change biology 20 (2), 544–554.
Vermeij, M., Frade, P., Jacinto, R., Debrot, A., Bak, R., 2007. Effects of reproductive mode on habitat-related differences in the population structure of eight Caribbean coral species. Mar. Ecol. Prog. Ser. 351, 91–102.
Wagenaar Hummelinck, P., 1977. Marine localities. Studies on the Fauna of Curacao and other Caribbean Islands 51 (1), 1–68.
Wang, M., Carver, J.J., Phelan, V.V., Sanchez, L.M., Garg, N., Peng, Y., Bandeira, N., 2016. Sharing and community curation of mass spectrometry data with Global Natural Products Social Molecular Networking. Nature biotechnology 34 (8), 828–837.
Wang, S., Vogt, R.D., Carstensen, J., Lin, Y., Feng, J., Lu, X., 2022. Riverine flux of dissolved phosphorus to the coastal sea may be overestimated, especially in estuaries of gated rivers: implications of phosphorus adsorption/desorption on suspended sediments. Chemosphere 287, 132206.
Weber, M., De Beer, D., Lott, C., Polerecky, L., Kohls, K., Abed, R.M., Ferdelman, T.G., Fabricius, K.E., 2012. Mechanisms of damage to corals exposed to sedimentation. Proc. Natl. Acad. Sci. 109 (24), E1558–E1567.
Wynne, S., 2017. Observational evidence of regional eutrophication in the Caribbean Sea and potential impacts on coral reef ecosystems and their management in Anguilla, BWI. Anguilla Fisheries and Marine Resources Research Bulletin 8 (08), 1–22.
Zhang, Z., Wang, Y., Chen, B., Lei, C., Yu, Y., Xu, N., Zhang, Q., Wang, T., Gao, W., Lu, T., 2022. Xenobiotic pollution affects transcription of antibiotic resistance and virulence factors in aquatic microcosms. Environ. Pollut. 306, 119396.
Zhao, F., Zhan, X., Xu, H., Zhu, G., Zou, W., Zhu, M., Kang, L., Guo, Y., Zhao, X., Wang, Z., 2022. New insights into eutrophication management: importance of temperature and water residence time. J. Environ. Sci. 111, 229–239.
Zheng, L.-W., Zhai, W.-D., Wang, L.-F., Huang, T., 2020. Improving the understanding of central Bohai Sea eutrophication based on wintertime dissolved inorganic nutrient budgets: roles of north Yellow Sea water intrusion and atmospheric nitrogen deposition. Environ. Pollut. 267, 115626.
Zweifler, A., O'leary, M., Morgan, K., Browne, N.K., 2021. Turbid coral reefs: past, present and future—a review. Diversity 13 (6), 251.